

# Diabatic analysis of the electronic states of hydrogen chloride

Rohana Liyanage<sup>a)</sup> and Robert J. Gordon

*Department of Chemistry (m/c 111), University of Illinois at Chicago, 845 West Taylor Street, Chicago, Illinois 60607-7061*

Robert W. Field

*Department of Chemistry, Massachusetts Institute of Technology, Cambridge, Massachusetts 02139*

(Received 1 June 1998; accepted 14 July 1998)

An effective Hamiltonian method was used to deperturb the  $(X^2\Pi_i)4p\sigma$  and  $(X^2\Pi_i)4p\pi$  Rydberg states and the  $V^1\Sigma^+$  valence state of HCl and DCl. A least-squares fit of the eigenvalues of the Hamiltonian to the experimental term energies was performed, and the zero-order diabatic characters of the basis states were determined. These deperturbed states were used to fit the observed  $\Lambda$ -splittings, to predict the energies of unknown states, to model spectroscopic intensity anomalies, and to explain the spin-orbit branching ratio for predissociation. © 1998 American Institute of Physics. [S0021-9606(98)00939-8]

## I. INTRODUCTION

Rydberg states of molecules with closed-shell ground states are described by the interaction of one Rydberg electron and one valence hole. This electron/hole combination gives rise to clusters of several closely spaced and strongly interacting states, producing an electronic spectrum of apparent complexity. The simplest way to analyze such spectra is with a diabatic picture, using a Hund's case (a) Hamiltonian to provide a convenient, zero-order description of the molecular eigenstates. This picture may be further simplified by insisting that all Rydberg states built on the same ion-hole electronic state have identical potential energy curves and molecular constants. In such a zero-order picture, the simple structure behind the apparent complexity of the spectrum is produced by the interactions between only two orbitals, expressed in terms of Coulomb and exchange integrals of the interelectronic repulsion operator.

Real molecules are more complex because of interactions between the zero-order states caused by terms in the Hamiltonian that are neglected in the diabatic picture. This complexity is only apparent, however. By understanding the nature of these interactions, it is possible to recover from the observed spectrum the underlying simplicity of the zero-order, electron/hole description of the molecule. Instead of dealing with the complex spectrum of many electronic states, it is sufficient to describe the molecule at an orbital level, considering only one- and two-electron interactions. Conversely, starting from a zero-order picture and knowing the values of all relevant coupling matrix elements of the Hamiltonian, it is possible to predict all desired observables relevant to both frequency and time domain experiments. In this paper we present an analysis of a representative case in which this minimalist view successfully accounts for a broad range of spectroscopic and dynamic properties of a molecule.

The molecule that we have chosen for this study is hy-

drogen chloride.<sup>1-3</sup> A simplifying property of this molecule is its atomlike nature. Most of its orbitals are dominated by Cl atomic orbitals whose properties (e.g., the spin-orbit coupling constant and the radial nodal structure) are well known. The equilibrium configuration of the ground ( $X^1\Sigma^+$ ) electronic state of HCl is  $4\sigma^2 5\sigma^2 2\pi^4$ , which corresponds to a closed-shell  $H^+Cl^-$  ionic structure. Promotion of an electron from a  $2\pi$  valence orbital to the  $6\sigma$  antibonding orbital (nominally a transition from a hydrogen  $1s$  orbital to a chlorine  $3p$  orbital) generates the  $a^3\Pi_i$  and  $A^1\Pi$  repulsive states. Promotion instead of an electron from a  $5\sigma$  valence orbital to the  $6\sigma$  antibonding orbital produces the repulsive  $t^3\Sigma_i^+$  and the bound  $V^1\Sigma^+$  valence states. The valence, or ion-pair state, has a covalent configuration at short internuclear distances and an ionic configuration at long distances. Promotion of these  $2\pi$  or  $5\sigma$  electrons to higher-lying orbitals results in Rydberg states with either an  $X^2\Pi_i(\sigma^2\pi^3)$  or an  $A^2\Sigma^+(\sigma\pi^4)$  ionic core. A primary issue is the strength of the interactions of the Rydberg electron with the hole in the partly filled ion core. In this paper we are concerned exclusively with Rydberg states having a ground state core, i.e., with an  $(X^2\Pi_i)n\ell/\lambda$  nominal configuration. The specific states that we will deal with are the  $V^1\Sigma^+$  valence state, the  $b^3\Pi_i$  and  $C^1\Pi$  Rydberg states, for which the promoted electron is in the  $4s\sigma$  orbital, the  $d^3\Pi_i$  and  $D^1\Pi$  Rydberg states with the promoted electron in the  $4p\sigma$  orbital, and the  $e^3\Sigma_i^+$ ,  $E^1\Sigma^+$ ,  $g^3\Sigma_i^-$ ,  $G^1\Sigma^+$ ,  $f^3\Delta_i$ , and  $F^1\Delta$  Rydberg states, where the promoted electron is in the  $4p\pi$  electron orbital.

The atomic character of HCl is evident from its adiabatic potential energy curves,<sup>4</sup> which consist of relatively compact clusters of states, with each cluster corresponding to occupancy of a different Rydberg orbital. The compactness of the clusters is symptomatic of the weakness of the interaction between core and Rydberg electrons, which is the primary basis for the apparent complexity of the spectrum. The simple atomic picture is complicated by the existence of different  $\Lambda$  states (where  $\Lambda$  is the projection of the orbital an-

<sup>a)</sup>Present address: Department of Chemistry, University of Utah, Salt Lake City, UT 84112.

gular momentum along the internuclear axis) and the interactions among them. Specific examples of perturbations, which were analyzed in previous papers, are  $\Lambda$ -doubling of the  $F^1\Delta$  state<sup>5</sup> and the  $J$ -dependent predissociation of the  $F^1\Delta$  state,<sup>5-7</sup> the  $E^1\Sigma^+$  state,<sup>7</sup> the  $g^3\Sigma_0^-$  state,<sup>8</sup> and the  $C^1\Pi$  state.<sup>9</sup> Our goal in this paper is to provide quantitative explanations for these perturbations in the spectra of HCl and DCI, and, in so doing, to uncover the underlying zero-order structure which could be used to account for other spectroscopic and dynamic effects.

## II. DEPERTURBATION SCHEME

The overall approach to this problem is to diagonalize an effective Hamiltonian matrix and to fit its eigenvalues to all of the observed term values of states in a particular energy region. In this section we review the method used for constructing this matrix and define the spectroscopic parameters that are fit to the data. Throughout, the notation is close to that used in the book by Lefebvre-Brion and Field.<sup>10</sup> We start by writing the Hamiltonian  $\mathcal{H}$  as the sum of three operators,

$$\mathcal{H} = \mathcal{H}^{\text{el}} + T^{\text{N}} + \mathcal{H}^{\text{el}}. \quad (1)$$

The first operator is the clamped-nuclei (Born–Oppenheimer) electronic Hamiltonian

$$\mathcal{H}^{\text{el}} = T^{\text{e}}(r) + V(r, R), \quad (2)$$

where  $T^{\text{e}}$  is the electronic kinetic energy,  $V(r, R)$  is the potential energy of the nuclei and electrons,  $R$  is the internuclear distance, and  $r$  represents the electronic coordinates. The potential energy can be broken into electron–nuclear, nuclear–nuclear, and electron–electron interactions,

$$V(r, R) = V^{\text{eN}}(r, R) + V^{\text{NN}}(R) + V^{\text{ee}}(r), \quad (3)$$

The second term in Eq. (1) is the nuclear kinetic energy operator,  $T^{\text{N}}$ , which consists of vibrational and rotational terms (see Ref. 10)

$$T^{\text{N}}(R, \theta, \phi) = T^{\text{VIB}}(R) + \mathcal{H}^{\text{ROT}}(R, \theta, \phi), \quad (4)$$

where  $\theta$  and  $\phi$  are the orientation angles of the bond axis ( $z$ ) relative to the laboratory coordinate system with its origin at the molecular center of mass. The rotational Hamiltonian may be further partitioned into terms containing the total angular momentum,  $\mathbf{J}$ , the electronic orbital angular momentum,  $\mathbf{L}$ , and the spin,  $\mathbf{S}$ ,

$$\begin{aligned} \mathcal{H}^{\text{ROT}} = & B(R)[(\mathbf{J}^2 - \mathbf{J}_z^2) + (\mathbf{L}^2 - \mathbf{L}_z^2) + (\mathbf{S}^2 - \mathbf{S}_z^2) \\ & + (\mathbf{L}^+ \mathbf{S}^- + \mathbf{L}^- \mathbf{S}^+) - (\mathbf{J}^+ \mathbf{S}^- + \mathbf{J}^- \mathbf{S}^+) \\ & - (\mathbf{J}^+ \mathbf{L}^- + \mathbf{J}^- \mathbf{L}^+)], \end{aligned} \quad (5)$$

where  $\mathbf{J}^{\pm}$ ,  $\mathbf{L}^{\pm}$ , and  $\mathbf{S}^{\pm}$  are ladder operators, and  $B$  is an  $R$ -dependent operator. The last term in Eq. (1) is the relativistic Hamiltonian,  $\mathcal{H}^{\text{rel}}$ , which includes the spin-orbit, spin-spin, and spin-rotation operators

$$\mathcal{H}^{\text{rel}} = \mathcal{H}^{\text{SO}} + \mathcal{H}^{\text{SS}} + \mathcal{H}^{\text{SR}}. \quad (6)$$

For all but the simplest systems, it is very difficult to diagonalize the full Hamiltonian directly. The usual starting point for calculating the eigenstates of  $\mathcal{H}$  is the Born–

Oppenheimer approximation,<sup>11</sup> in which the nuclei are assumed to be clamped at internuclear distance  $R$ , so that the eigenfunctions of  $\mathcal{H}^{\text{el}}$  may be factored into products of electronic functions,  $\Phi_i(r; R)$ , and nuclear (vibration–rotation) functions,  $\chi_{v,J}(R)$ . The former are obtained by diagonalizing either  $\mathcal{H}^{\text{el}}$  or  $\mathcal{H}^{\text{el}} + \mathcal{H}^{\text{SO}}$  by means of a suitable variational calculation at a grid of internuclear distances. In the more common nonrelativistic treatment used in this paper,  $\mathcal{H}^{\text{el}}$  is diagonalized, yielding as its eigenfunctions the adiabatic wave functions  $\Phi_i^{\text{ad}}(r; R)$  and as its ( $R$ -dependent) eigenvalues the nonrotating Born–Oppenheimer potential energy curves,  $V_i^{\text{BO}}(R)$ . The adiabatic potential energy curves,  $V_i^{\text{ad}}(R)$ , may be obtained by adding  $\langle \Phi_i^{\text{ad}} | T^{\text{N}} | \Phi_i^{\text{ad}} \rangle_r$  diagonal matrix elements to  $V_i^{\text{BO}}(R)$ . (The subscript  $r$  indicates integration over all electronic coordinates.)

The adiabatic (or Born–Oppenheimer) potential energy curves may be used to construct a set of coupled nuclear Schrödinger equations, which may in turn be solved for the total energy and the adiabatic nuclear wave functions,  $\chi_{v,J}^{\text{ad}}(R)$ . In order to uncouple these equations we define the projection operator  $P$ , such that

$$PT^{\text{N}} = \sum_i |\phi_i^{\text{ad}}\rangle_r T^{\text{N}} \langle \phi_i^{\text{ad}}|, \quad (7)$$

which is used to further partition the nuclear kinetic energy operator,

$$T^{\text{N}} = PT^{\text{VIB}} + (1 - P)T^{\text{VIB}} + \mathcal{H}^{\text{ROT}}. \quad (8)$$

In the Born–Oppenheimer approximation the  $(1 - P)T^{\text{VIB}}$  operator, which is nondiagonal in the  $\chi_{v,J}^{\text{ad}} \phi_i^{\text{ad}}$  basis, is neglected. The remaining diagonal terms in  $T^{\text{N}}$  lead to the uncoupled nuclear Schrödinger equation

$$\langle \phi_i^{\text{ad}} | PT^{\text{VIB}} + \mathcal{H}^{\text{ROT}} + V_i^{\text{ad}}(R) - E | \phi_i^{\text{ad}} \rangle_r \chi_{v,J}^{\text{ad}}(R) = 0, \quad (9a)$$

or

$$[T^{\text{VIB}} + \langle \mathcal{H}^{\text{ROT}} \rangle_r + V_i^{\text{ad}}(R) - E] \chi_{v,J}^{\text{ad}}(R) = 0, \quad (9b)$$

which can be solved for  $E$  and  $\chi_{v,J}^{\text{ad}}(R)$ .

Because configuration interaction is built into  $\mathcal{H}^{\text{el}}$ , the adiabatic (or Born–Oppenheimer) potential curves for states of the same symmetry necessarily repel each other. Instead of using these noncrossing curves and the associated adiabatic electronic and vibrational wave functions, we choose to transform to a diabatic (crossing) basis, following the phenomenological procedure described in Ref. 10. The assumptions required for this transformation are (i) the existence of a complete set of diabatic wave functions,  $\Phi_i^{\text{d}}(r; R)$ , which are linear combinations of  $\Phi_i^{\text{ad}}(r; R)$  [Eq. (2.3.13) of Ref. 10 for the two-state case], and (ii) the existence of a set of well-behaved, intersecting, diabatic potential energy curves,  $V_i^{\text{d}}(R)$  [ $E_i^{\text{d}}(R)$  in Eq. (2.3.12) of Ref. 10]. In the two-state limit, these cross at internuclear distance  $R_C$ . Because by assumption  $V_1^{\text{d}}(R_C) = V_2^{\text{d}}(R_C)$ , the coupling matrix element in the diabatic basis,  $H_{12}^{\text{e}}(R) \equiv \langle \Phi_1^{\text{d}} | \mathcal{H}^{\text{el}} | \Phi_2^{\text{d}} \rangle_r$ , has the absolute value  $1/2 | V_1^{\text{ad}}(R_C) - V_2^{\text{ad}}(R_C) |$  at the crossing point.<sup>12</sup> An auxiliary assumption, that  $H_{12}^{\text{e}}(R)$  is independent of  $R$  in the interaction region, completes the prescription for transforming from one basis to the other. The resulting diabatic poten-

tial energy curves may be inserted into the nuclear Schrödinger equation to solve for the total energy and the diabatic nuclear wave functions,  $\chi_{v,J}^d(R)$ .

The adiabatic and diabatic wave functions are alternative zero-order approximations of the true eigenstates. Both form a complete basis set in which the eigenstates may be expanded. The advantage of the diabatic model is its simplicity, especially when the off-diagonal matrix elements are all small relative to typical vibrational spacings within each electronic state. The diabatic eigenfunctions are Hund's case (a) wave functions,  $|\Omega\Lambda\Sigma\rangle$ , where  $\Lambda$  and  $\Sigma$  are, respectively, the projections of  $\mathbf{L}$  and  $\mathbf{S}$  along the internuclear axis, and  $\Omega = \Lambda + \Sigma$ . Our task is to express  $\mathcal{H}$  as a matrix in this representation. In constructing this matrix, it is convenient to partition  $\mathcal{H}$  into a zero-order term,  $\mathcal{H}_0$ , given by

$$\begin{aligned} \mathcal{H}_0 = & T^{\text{VIB}} + V^d(R) + B(R)\langle \mathbf{J}^2 - \mathbf{J}_z^2 \rangle_r + B(R)\langle \mathbf{S}^2 - \mathbf{S}_z^2 \rangle_r \\ & + B(R)\langle \mathbf{L}^2 - \mathbf{L}_z^2 \rangle_r + A_{S,\Lambda}(R)\langle \mathbf{L}_z \mathbf{S}_z \rangle_r, \end{aligned} \quad (10)$$

and a nondiagonal perturbation term,

$$\begin{aligned} \mathcal{H}' = & \mathcal{H}^{\text{el}} + B(R)\langle \mathbf{L}^+ \mathbf{S}^- + \mathbf{L}^- \mathbf{S}^+ \rangle_r \\ & - B(R)\langle \mathbf{J}^+ \mathbf{L}^- + \mathbf{J}^- \mathbf{L}^+ \rangle_r - B(R)\langle \mathbf{J}^+ \mathbf{S}^- + \mathbf{J}^- \mathbf{S}^+ \rangle_r \\ & + (\mathcal{H}^{\text{SO}} - A_{S,\Lambda,S',\Lambda'}(R))\langle \mathbf{L}_z \mathbf{S}_z \rangle_r + \mathcal{H}^{\text{SS}} + \mathcal{H}^{\text{SR}}, \end{aligned} \quad (11)$$

where the spin-orbit operators  $A_{S,\Lambda}(R)$  and  $A_{S,\Lambda,S',\Lambda'}(R)$  vary slowly with  $R$ .

By definition,  $\mathcal{H}_0$  is diagonal in this representation, and its eigenvalues are the energies of the zero-order diabatic states. We assign a single, leading electronic configuration to each eigenstate, and write down analytic expressions for the matrix elements of  $\mathcal{H}'$  in terms of a set of physically motivated parameters. The resulting effective Hamiltonian,  $\mathcal{H}^{\text{eff}}$ , is diagonalized, and its parameters are optimized by fitting the calculated line positions to the ones in the observed spectrum. The designation "effective" is used to indicate that the effects of states omitted from the basis set may be included by the use of a Van Vleck transformation, which introduces additional effective molecular constants [see Ref. 10 and Eqs. (25)–(27) below]. What emerges from this calculation is a representation of the true eigenstates as linear combinations of zero-order, diabatic, wave functions. We refer to the squares of the coefficients in this expansion as the "diabatic state characters" of the observed states.

To express the matrix elements of  $\mathcal{H}^{\text{eff}}$  it is necessary to evaluate the molecular constants that appear in each of its terms. One way to do this is to use a traditional set of phenomenological parameters for each of the electronic states and for the interactions between the states. To do so here would require over 100 adjustable parameters. This approach is not only unacceptably cumbersome, it fails to provide the simple zero-order picture that we seek. Instead, we introduce a much smaller set of parameters consisting of one- and two-electron matrix elements among the two or three incompletely filled orbitals which we assume to be common to all the states of interest.

Calculation of the matrix elements of the effective Hamiltonian is discussed in detail in Ref. 10. In what follows

we collect the key results and indicate the approximations that have been made in our analysis. Consider first the contribution of each term in Eq. (10) to the expectation value of  $\mathcal{H}_0$ . The matrix elements of the first two terms are evaluated as

$$\begin{aligned} \langle \Omega\Lambda\Sigma vJ | T^{\text{VIB}} + V^d(R) | \Omega\Lambda\Sigma vJ \rangle \\ = E_{S,\Lambda} + (v' + 1/2)\omega_e - (v' + 1/2)^2\omega_e x_e \\ + (v' + 1/2)^3\omega_e y_e + [B_e - \alpha_e(v' + 1/2)]X, \end{aligned} \quad (12)$$

where  $E_{S,\Lambda}$  is the electronic term value (i.e., the potential energy minimum of the upper electronic state at internuclear separation  $R'_e$  relative to the zero of energy of the ground state at  $R''_e$ , written in spectroscopic notation as  $T_e$ ),  $v'$  is the vibrational quantum number,  $X = J'(J' + 1)$ , and the other symbols have their usual meaning.<sup>13</sup> In cases where only the ground vibrational level is included,  $\langle T^{\text{VIB}} \rangle$  is absorbed into  $E_{S,\Lambda}$ . The third and fourth terms in Eq. (10) have an expectation value

$$\begin{aligned} \langle \Omega\Lambda\Sigma vJ | \mathcal{H}^{\text{ROT}} | \Omega\Lambda\Sigma vJ \rangle \\ = B_{v,S,\Lambda}(X - \Omega^2 + S(S + 1) - \Sigma^2), \end{aligned} \quad (13)$$

where  $B_{v,S,\Lambda} = \langle \Omega\Lambda\Sigma v | B(R) | \Omega\Lambda\Sigma v \rangle$ .<sup>14</sup> In addition, a contribution from centrifugal distortion, incorporating the effects of  $\Delta v \neq 0$  matrix elements of  $B(R)$  (within each electronic state) into the  $\Delta v = 0$  blocks in the Hamiltonian, is included in  $\langle \mathcal{H}^{\text{ROT}} \rangle$ .<sup>10</sup> Because the expectation value of  $\mathbf{L}^2$  is undefined, the contribution of the fifth term is incorporated into  $E_{S,\Lambda}$ . The last term in Eq. (10) is the diagonal part of the spin-orbit operator; its expectation value is

$$\langle \Omega\Lambda\Sigma vJ | A_{S,\Lambda} \mathbf{L}_z \mathbf{S}_z | \Omega\Lambda\Sigma vJ \rangle_r = A_{v,S,\Lambda} \Lambda \Sigma, \quad (14)$$

where  $A_{v,S,\Lambda} = \langle \Omega\Lambda\Sigma v | A_{S,\Lambda}(R) | \Omega\Lambda\Sigma v \rangle$ .<sup>14</sup>

We turn now to the terms in Eq. (11), which are responsible for interactions between different zero-order states. The first term is the interelectronic repulsion, which is responsible for configuration interaction between states of the same  $S, \Lambda$  symmetry. Here it produces the Rydberg–valence interaction between the  $E^1\Sigma^+$  and  $V^1\Sigma^+$  states. Its matrix element is the product of a constant electronic term  $H_{E-V}^e$  and a vibrational overlap factor. The second term is a spin-electronic operator, which connects states with different values of  $\Lambda$  and  $\Sigma$  but with the same value of  $\Omega$ . The third term is the  $\mathbf{L}$ -uncoupling operator, which connects states with different  $\Lambda$  and  $\Omega$  but the same  $S$  and  $\Sigma$ . The fourth term is the  $\mathbf{S}$ -uncoupling operator, which connects states with different  $\Sigma$  and  $\Omega$ . In evaluating the matrix elements of  $\mathbf{J}^\pm$ , one must take into account the consequences of the anomalous commutation rules (i.e., the raising and lowering roles of  $\mathbf{J}^+$  and  $\mathbf{J}^-$  are interchanged). In evaluating the matrix elements of  $\mathbf{L}^\pm$  (Ref. 10), we correct for the fact that the actual Rydberg electrons are not in states of pure orbital angular momentum,  $l$ . To account phenomenologically for the actual  $l$ -mixing (caused by the nonspherical nature of the ion core and also by the choice of the coordinate origin at the center of mass rather than at the Cl atomic nucleus),<sup>15,16</sup> we introduce a parameter  $b$ ,

$$b = \langle 4p\pi | l^\pm | 4p\sigma \rangle. \quad (15)$$

In the limit of “pure-precession” of a  $p$ -orbital,  $b = (l(l+1))^{1/2} = 2^{1/2}$ .

The fifth term in Eq. (11) is the nondiagonal part of the spin-orbit operator, which may be written in terms of single-electron operators<sup>10</sup> as

$$H^{SO} = \hat{\mathbf{a}}_{\Pi} \mathbf{l}_{\Pi} s_{\Pi} + \hat{\mathbf{a}}_{\Pi}^r \mathbf{l}_{\Pi}^r s_{\Pi}^r + 1/2 \hat{\mathbf{a}}_{\Pi} (\mathbf{l}_{\Pi}^+ s_{\Pi}^- + \mathbf{l}_{\Pi}^- s_{\Pi}^+) + 1/2 \hat{\mathbf{a}}_{\Pi}^r (\mathbf{l}_{\Pi}^{r+} s_{\Pi}^{r-} + \mathbf{l}_{\Pi}^{r-} s_{\Pi}^{r+}), \quad (16)$$

where  $\hat{\mathbf{a}}_{\Pi}$  and  $\hat{\mathbf{a}}_{\Pi}^r$  operate on the core and Rydberg electron, respectively. In general,  $\hat{\mathbf{a}}$  is an operator that acts only on the radial part of the wave function. The operator  $\hat{\mathbf{a}}_i$  is defined as<sup>10</sup>

$$\hat{\mathbf{a}}_i = \sum_K (\alpha^2/2) (Z_{\text{eff}K}/r_{iK}^3) \mathbf{l}_{iK}, \quad (17)$$

where  $\mathbf{l}_{iK}$  is the orbital angular momentum of electron  $i$  about nucleus  $K$ ,  $Z_{\text{eff}K}$  is the effective charge of the  $K$ th nucleus, and  $\alpha$  is the fine-structure constant.

The sixth term in Eq. (11) is the spin-spin operator,<sup>10</sup>

$$\mathcal{H}^{SS} = C_{\Lambda} (\mathbf{S}^2 - 3\mathbf{S}_z^2). \quad (18)$$

The diagonal matrix element of  $\mathcal{H}^{SS}$  is

$$\langle \Omega \Lambda S \Sigma | \mathcal{H}^{SS} | \Omega \Lambda S \Sigma \rangle = C_{\Lambda} [S(S+1) - 3\Sigma^2]. \quad (19)$$

The nondiagonal matrix elements of this operator are small and were ignored in this work. Finally, the last term in Eq. (11) is the spin-rotation operator, which has the effective form<sup>10</sup>

$$\mathcal{H}^{SR} = \gamma (\mathbf{J} - \mathbf{L} - \mathbf{S}) \cdot \mathbf{S}. \quad (20)$$

The diagonal matrix elements of  $\mathcal{H}^{SR}$  are

$$\langle \Omega \Lambda S \Sigma | \mathcal{H}^{SR} | \Omega \Lambda S \Sigma \rangle = \gamma [\Sigma^2 - S(S+1)]. \quad (21)$$

The off-diagonal part of  $\mathcal{H}^{SR}$  connects some of the same basis states as the spin-orbit and  $\mathbf{S}$ -uncoupling operators, and has the same quantum number dependencies, but with an opposite sign.<sup>17</sup>

### III. DEPERTURBATION OF THE SPECTRUM OF HYDROGEN CHLORIDE

The effective Hamiltonians for HCl and DCl were constructed using the methods outlined in the previous section. The two-electron Slater determinants for the states included in our analysis are listed in Table I, and their matrix elements are listed in Table II. Included in our analysis are the  $(X^2\Pi_i)4p\sigma$  and  $(X^2\Pi_i)4p\pi$  Rydberg states and the  $V^1\Sigma^+(v'=8-12$  for HCl and  $v'=12-15$  for DCl) valence state, spanning the energy range of 81 600–85 300 for HCl and 82 900–85 300  $\text{cm}^{-1}$  for DCl.

Excluded from our basis set are a number of states that are so broadened by predissociation that they have not been observed in the spectra recorded so far. Important examples are the  $b^3\Pi(v'=3)$  and the  $C^1\Pi_i(v'=2)$  states<sup>9</sup> of HCl, which couple to the  $F^1\Delta$  and  $f^3\Delta_i$  states and are the cause of a  $J$ -dependent intensity loss in the ionization signal.<sup>5-7</sup> Because the present fit is primarily of the observed term values, it is necessary to assess what effect the unseen (and otherwise ignored) states might have on the energy levels.

TABLE I. Zero-order wave functions.

Electronic State	Wave function
$E^1\Sigma_0^+$	$1/2[ \pi^+\alpha\pi_r^-\beta\rangle -  \pi^+\beta\pi_r^-\alpha\rangle -  \pi^-\beta\pi_r^+\alpha\rangle +  \pi^-\alpha\pi_r^+\beta\rangle]$
$g^3\Sigma_0^-$	$1/2[ \pi^+\alpha\pi_r^-\beta\rangle +  \pi^+\beta\pi_r^-\alpha\rangle -  \pi^-\beta\pi_r^+\alpha\rangle -  \pi^-\alpha\pi_r^+\beta\rangle]$
$g^3\Sigma_{\pm 1}^-$	$2^{-1/2}[ \pi^+\alpha\pi_r^-\alpha\rangle -  \pi^-\alpha\pi_r^+\alpha\rangle]$ or $2^{-1/2}[ \pi^+\beta\pi_r^-\beta\rangle -  \pi^-\beta\pi_r^+\beta\rangle]$
$D^1\Pi_{\pm 1}$	$2^{-1/2}[ \pi^+\alpha\sigma_r\beta\rangle -  \pi^+\beta\sigma_r\alpha\rangle]$ or $2^{-1/2}[ \pi^-\alpha\sigma_r\beta\rangle -  \pi^-\beta\sigma_r\alpha\rangle]$
$d^3\Pi_{\pm 1}$	$2^{-1/2}[ \pi^+\alpha\sigma_r\beta\rangle +  \pi^+\beta\sigma_r\alpha\rangle]$ or $2^{-1/2}[ \pi^-\beta\sigma_r\alpha\rangle +  \pi^-\alpha\sigma_r\beta\rangle]$
$d^3\Pi_{\pm 2}$	$ \pi^+\alpha\sigma_r\alpha\rangle$ or $ \pi^-\beta\sigma_r\beta\rangle$
$d^3\Pi_{\pm 0}^a$	$ \pi^+\beta\sigma_r\beta\rangle$ or $ \pi^-\alpha\sigma_r\alpha\rangle$
$f^3\Delta_{\pm 1}$	$ \pi^+\beta\pi_r^+\beta\rangle$ or $ \pi^-\alpha\pi_r^-\alpha\rangle$
$f^3\Delta_{\pm 2}$	$2^{-1/2}[ \pi^+\alpha\pi_r^+\beta\rangle +  \pi^+\beta\pi_r^+\alpha\rangle]$ or $2^{-1/2}[ \pi^-\beta\pi_r^-\alpha\rangle +  \pi^-\alpha\pi_r^-\beta\rangle]$
$f^3\Delta_{\pm 3}$	$ \pi^+\alpha\pi_r^+\alpha\rangle$ or $ \pi^-\beta\pi_r^-\beta\rangle$
$F^1\Delta_{\pm 2}$	$2^{-1/2}[ \pi^+\alpha\pi_r^+\beta\rangle -  \pi^+\beta\pi_r^+\alpha\rangle]$ or $2^{-1/2}[ \pi^-\beta\pi_r^-\alpha\rangle -  \pi^-\alpha\pi_r^-\beta\rangle]$
$G^1\Sigma_0^-$	$1/2[ \pi^+\alpha\pi_r^-\beta\rangle -  \pi^+\beta\pi_r^-\alpha\rangle +  \pi^-\beta\pi_r^+\alpha\rangle -  \pi^-\alpha\pi_r^+\beta\rangle]$
$e^3\Sigma_0^+$	$1/2[ \pi^+\alpha\pi_r^-\beta\rangle +  \pi^+\beta\pi_r^-\alpha\rangle +  \pi^-\beta\pi_r^+\alpha\rangle +  \pi^-\alpha\pi_r^+\beta\rangle]$
$e^3\Sigma_{\pm 1}^+$	$2^{-1/2}[ \pi^+\alpha\pi_r^-\alpha\rangle +  \pi^-\alpha\pi_r^+\alpha\rangle]$ or $2^{-1/2}[ \pi^+\beta\pi_r^-\beta\rangle +  \pi^-\beta\pi_r^+\beta\rangle]$

<sup>a</sup>The wave functions for  $e/f$  lambda-type doublets of the  $d^3\Pi_0$  state are linear combinations of these Slater determinants. (See Ref. 10.)

Near degenerate vibrational levels of unseen states could conceivably cause large  $J$ -dependent level shifts of the observed states. From second-order perturbation theory, the energy level shift is given by

$$\delta E \sim V^2/\Delta E_J, \quad (22)$$

where  $V$  is a coupling matrix element and  $\Delta E_J$  is the difference between same- $J$  term values of the interacting states. The width of the perturbed state is given by<sup>10</sup>

$$\Gamma_E \sim (V/\Delta E_J)^2 \Gamma_{b,C}, \quad (23)$$

where the mixing fraction,  $(V/\Delta E_J)^2$ , expresses how the width of the perturbing state is borrowed by the perturbed state, and  $\Gamma_{b,C}$  is the width of the perturbing state. Substituting Eq. (22) into Eq. (23) gives

$$\delta E \sim \Gamma_E \Delta E_J / \Gamma_{b,C}. \quad (24)$$

From the widths of the observed spectral lines we estimate that  $\Gamma_E \approx 0.3 \text{ cm}^{-1}$ , and, inasmuch as the perturbing levels have not been observed, we estimate that  $\Gamma_{b,C} > 100 \text{ cm}^{-1}$ . For  $\Delta E_J/\Gamma_{b,C} < 1$ , the level shifts produced by nearby vibrational levels are accordingly negligible. Remote vibrational levels and continua of unseen states, however, can collectively produce appreciable level shifts that mimic the effects of the spin-spin and spin-rotation interactions. These effects are absorbed into large effective spin-spin ( $C$ ) and spin-rotation ( $\gamma$ ) constants.

States excluded from our basis set are the above-mentioned  $b^3\Pi_i$  and  $C^1\Pi$  states (for which the  $v' > 1$  levels required for our energy range are absent in the spectrum), the  $e^3\Sigma_{0,1}^+$  state (which has never been observed), the  $J' = 0-8$  levels of the  $G^1\Sigma^-$  state (which are not seen in the spectrum), and the  $t^3\Sigma^+$ ,  $A^1\Pi$ , and  $a^3\Pi$  continuum states.

TABLE II. Matrix elements of the effective Hamiltonian.

Definitions of some integrals and constants<sup>a</sup>

$$\begin{aligned}
B_{v',v''} &= \langle v' | \hbar^2 / (2\mu R^2) | v'' \rangle \\
a_{\Pi} &= \langle \sigma^2 \pi^3 | \hat{\mathbf{a}}_{\Pi} | \sigma^2 \pi^3 \rangle \text{ or } \langle \pi^{-1} | \hat{\mathbf{a}}_{\Pi} | \pi^{-1} \rangle \\
a_{\Pi}^r &= \langle 4p\pi | \hat{\mathbf{a}}_{\Pi}^r | 4p\pi \rangle \text{ or } \langle \pi_r | \hat{\mathbf{a}}_{\Pi} | \pi_r \rangle \\
A_{\Pi} &= a_{\Pi}/2 \\
A_{\Delta} &= (a_{\Pi} + a_{\Pi}^r)/4 \\
a_+ &= \langle 4p\pi | \hat{\mathbf{a}}_{\Pi}^+ | 4p\pi \rangle \text{ or } \langle \pi_r | \hat{\mathbf{a}}_{\Pi}^+ | \sigma_r \rangle \\
b &= \langle 4p\pi | 1^+ | 4p\pi \rangle
\end{aligned}$$

Diagonal matrix elements<sup>b</sup>

$$\begin{aligned}
\langle {}^1\Sigma_0^+ | H | {}^1\Sigma_0^+ \rangle &= E_{1\Sigma} + B_{1\Sigma} X - D_{1\Sigma} X^2 \\
\langle {}^1\Sigma_0^- | H | {}^1\Sigma_0^- \rangle &= E_{1\Sigma} - B_{1\Sigma} X - D_{1\Sigma} X^2 \\
\langle {}^3\Sigma_0^- | H | {}^3\Sigma_0^- \rangle &= E_{3\Sigma} - B_{3\Sigma} (X+2) - 2\gamma_{\Sigma} + 2C_{\Sigma} - D_{3\Sigma} (X^2 + 8X + 4) \\
\langle {}^3\Sigma_1^-, e | H | {}^3\Sigma_1^-, e \rangle &= E_{3\Sigma} - B_{3\Sigma} X - \gamma_{\Sigma} - C_{\Sigma} - D_{3\Sigma} (X^2 + 2X) \\
\langle {}^3\Sigma_1^-, f | H | {}^3\Sigma_1^-, f \rangle &= E_{3\Sigma} - B_{3\Sigma} X - \gamma_{\Sigma} - C_{\Sigma} - D_{3\Sigma} X^2 \\
\langle D^{-1}\Pi | H | D^{-1}\Pi \rangle &= E_{\Pi} + B_{\Pi} (X-1) - D_{\Pi} (X^2 - 2X + 1) \\
\langle d^{-3}\Pi_2 | H | d^{-3}\Pi_2 \rangle &= E_{3\Pi} + B_{3\Pi} (X-3) + A_{\Pi} - C_{\Pi} - \gamma_{\Pi} - D_{3\Pi} (X^2 - 4X + 5) + B_0^+ (X-2) \\
\langle d^{-3}\Pi_1, e | H | d^{-3}\Pi_1, e \rangle &= E_{3\Pi} + B_{3\Pi} (X+1) + 2C_{\Pi} - 2\gamma_{\Pi} - D_{3\Pi} (X^2 + 6X - 3) + A_0^+ \\
\langle d^{-3}\Pi_1, f | H | d^{-3}\Pi_1, f \rangle &= E_{3\Pi} + B_{3\Pi} (X+1) + 2C_{\Pi} - 2\gamma_{\Pi} - D_{3\Pi} (X^2 + 6X - 3) + A_0^+ + 2B_0^+ X \\
\langle d^{-3}\Pi_0, e | H | d^{-3}\Pi_0, e \rangle &= E_{3\Pi} + B_{3\Pi} (X+1) - A_{\Pi} - C_{\Pi} - \gamma_{\Pi} - D_{3\Pi} (X^2 + 4X + 1) + B_0^+ X \\
\langle d^{-3}\Pi_0, f | H | d^{-3}\Pi_0, f \rangle &= E_{3\Pi} + B_{3\Pi} (X+1) - A_{\Pi} - C_{\Pi} - \gamma_{\Pi} - D_{3\Pi} (X^2 + 4X + 1) + B_0^+ X + 2A_0^+ \\
\langle f^{-3}\Delta_1 | H | f^{-3}\Delta_1 \rangle &= E_{3\Delta} + B_{3\Delta} X - 2A_{\Delta} - C_{\Delta} - \gamma_{\Delta} - D_{3\Delta} (X^2 + 2X - 4) \\
\langle f^{-3}\Delta_2 | H | f^{-3}\Delta_2 \rangle &= E_{3\Delta} + B_{3\Delta} (X-2) + 2C_{\Delta} - 2\gamma_{\Delta} - D_{3\Delta} (X^2 - 12) \\
\langle f^{-3}\Delta_3 | H | f^{-3}\Delta_3 \rangle &= E_{3\Delta} + B_{3\Delta} (X-8) + 2A_{\Delta} - C_{\Delta} - \gamma_{\Delta} - D_{3\Delta} (X^2 - 14X + 52) \\
\langle F^{-1}\Delta_2 | H | F^{-1}\Delta_2 \rangle &= E_{1\Delta} + B_{1\Delta} (X-4) - D_{1\Delta} (X^2 - 8X + 16) \\
\langle V^{-1}\Sigma_0^+, v' | H | V^{-1}\Sigma_0^+, v' \rangle &= T_0 + (v' + 1/2)\omega_e - (v' + 1/2)^2\omega_e x_e + (v' + 1/2)^3\omega_e y_e \\
&\quad + [B_e - \alpha_v (v' + 1/2)]X - D_v X^2
\end{aligned}$$

Off-diagonal matrix elements<sup>c</sup>

## Rydberg-Rydberg interactions:

$$\begin{aligned}
\langle {}^3\Sigma_1^- | H | {}^3\Sigma_0^- \rangle &= -2B_{v',v''} X^{1/2} + \gamma_{\Sigma} X^{1/2} + 4D_{3\Sigma} (X+1) X^{1/2} & [B_{v',v''} = B_{3\Sigma}] \\
\langle {}^3\Sigma_1^- | H | {}^3\Pi_1 \rangle &= -\frac{1}{4} a^+ \langle 0|0 \rangle - b B_{v',v''} & [B_{v',v''} = 9.85, \langle 0|0 \rangle = 0.9897] \\
\langle {}^3\Sigma_1^- | H | {}^1\Pi_1 \rangle &= \frac{1}{4} a^+ \langle 0|0 \rangle & [\langle 0|0 \rangle = 0.9846] \\
\langle {}^3\Sigma_1^- | H | {}^3\Pi_2 \rangle &= -2^{-1/2} b B_{v',v''} (X-2)^{1/2} & [B_{v',v''} = 9.85] \\
\langle {}^3\Sigma_1^- | H | {}^3\Pi_0 \rangle &= -2^{-1/2} b B_{v',v''} X^{1/2} & [B_{v',v''} = 9.85] \\
\langle {}^3\Sigma_0^- | H | {}^3\Pi_1 \rangle &= -b B_{v',v''} X^{1/2} & [B_{v',v''} = 9.85] \\
\langle {}^3\Sigma_0^- | H | {}^3\Pi_0 \rangle &= -2^{-1/2} a^+ \langle 0|0 \rangle - 2^{1/2} b B_{v',v''} & [B_{0,0} = 9.87, \langle 0|0 \rangle = 0.987] \\
\langle {}^1\Sigma_0^+ | H | {}^1\Pi_1 \rangle &= -b B_{v',v''} X^{1/2} & [B_{v',v''} = 9.35] \\
\langle {}^1\Sigma_0^+ | H | {}^3\Pi_0 \rangle &= 2^{-3/2} a^+ \langle 0|0 \rangle & [\langle 0|0 \rangle = 0.9898] \\
\langle {}^1\Sigma_0^+ | H | {}^3\Sigma_0^- \rangle &= \frac{1}{2} (a_{\Pi} + a_{\Pi}^r) \langle 0|0 \rangle & [\langle 0|0 \rangle = 0.9967] \\
\langle {}^1\Sigma_0^- | H | {}^1\Pi_1 \rangle &= b B_{v',v''} X^{1/2} & [B_{v',v''} = 9.35] \\
\langle {}^1\Sigma_0^- | H | {}^3\Pi_0 \rangle &= -2^{-3/2} a^+ \langle 0|0 \rangle & [\langle 0|0 \rangle = 0.9898] \\
\langle {}^3\Pi_1, e | H | {}^3\Pi_0, e \rangle &= (2X)^{1/2} [-B_{v',v''} + \frac{1}{2}\gamma_{\Pi} + 2(X+1)D_{3\Pi} + B_1^+] & [B_{v',v''} = B_{3\Pi}] \\
\langle {}^3\Pi_1, f | H | {}^3\Pi_0, f \rangle &= (2X)^{1/2} [-B_{v',v''} + \frac{1}{2}\gamma_{\Pi} + 2(X+1)D_{3\Pi} - 3B_1^+] & [B_{v',v''} = B_{3\Pi}] \\
\langle {}^3\Pi_1 | H | {}^1\Pi_1 \rangle &= \frac{1}{2} a_{\Pi} \langle 0|0 \rangle & [\langle 0|0 \rangle = 9521] \\
\langle {}^3\Pi_1 | H | {}^3\Pi_2 \rangle &= [2(X-2)]^{1/2} [-B_{v',v''} + \gamma_{\Pi}/2 + (X-1)D_{3\Pi} + B_1^+] & [B_{v',v''} = B_{3\Pi}] \\
\langle {}^3\Pi_2, e | H | {}^3\Pi_0, e \rangle &= [X(X-2)]^{1/2} [2D_{3\Pi} - B_0^+] \\
\langle {}^3\Pi_2, f | H | {}^3\Pi_0, f \rangle &= [X(X-2)]^{1/2} [2D_{3\Pi} + B_0^+] \\
\langle {}^3\Pi_1 | H | {}^3\Delta_1 \rangle &= 2^{-1/2} a^+ \langle 0|0 \rangle + 2^{1/2} b B_{v',v''} & [B_{v',v''} = 9.96, \langle 0|0 \rangle = 0.999] \\
\langle {}^3\Pi_1 | H | {}^3\Delta_2 \rangle &= -b B_{v',v''} (X-2)^{1/2} & [B_{v',v''} = 9.96] \\
\langle {}^3\Pi_0 | H | {}^3\Delta_1 \rangle &= -b B_{v',v''} X^{1/2} & [B_{v',v''} = 9.96] \\
\langle {}^3\Pi_2 | H | {}^3\Delta_3 \rangle &= -b B_{v',v''} (X-6)^{1/2} & [B_{v',v''} = 9.96] \\
\langle {}^3\Pi_2 | H | {}^3\Delta_1 \rangle &= -b B_{v',v''} (X-2)^{1/2} & [B_{v',v''} = 9.96] \\
\langle {}^3\Pi_2 | H | {}^3\Delta_2 \rangle &= 2^{-1/2} a^+ \langle 0|0 \rangle + 2^{1/2} b B_{v',v''} & [B_{v',v''} = 9.96, \langle 0|0 \rangle = 0.99] \\
\langle {}^3\Pi_2 | H | {}^1\Delta_2 \rangle &= 2^{-3/2} a^+ \langle 0|0 \rangle & [\langle 0|0 \rangle = 0.998] \\
\langle {}^1\Pi_1 | H | {}^1\Delta_2 \rangle &= -b B_{v',v''} (X-2)^{1/2} & [B_{v',v''} = 9.26] \\
\langle {}^1\Pi_1 | H | {}^3\Delta_1 \rangle &= -2^{-3/2} a^+ \langle 0|0 \rangle & [\langle 0|0 \rangle = 0.9638] \\
\langle {}^3\Delta_1 | H | {}^3\Delta_2 \rangle &= -B_{v',v''} [2(X-2)]^{1/2} + \gamma_{\Delta} [(X-2)/2]^{1/2} - 2D_{3\Delta} [2(X-2)]^{1/2} (X-1) & [B_{v',v''} = B_{3\Delta}] \\
\langle {}^3\Delta_3 | H | {}^3\Delta_2 \rangle &= -B_{v',v''} [2(X-6)]^{1/2} + \gamma_{\Delta} [(X-6)/2]^{1/2} + 2D_{3\Delta} [2(X-6)]^{1/2} (X-5) & [B_{v',v''} = B_{3\Delta}] \\
\langle {}^1\Delta_2 | H | {}^3\Delta_2 \rangle &= \frac{1}{2} (a_{\Pi} - a_{\Pi}^r) \langle 0|0 \rangle & [\langle 0|0 \rangle = 0.998]
\end{aligned}$$

## Rydberg-valence interaction:

$$\langle V^{-1}\Sigma_0^+, v' | H | E^{-1}\Sigma_0^+, v' = 0 \rangle = H_{E-v} \langle v' | 0 \rangle$$

$$v' = 8-12 \text{ for HCl and } v' = 12-15 \text{ for DCI}$$

<sup>a</sup> $\pi^{-1}$  represents the core.<sup>b</sup> $X = J'(J' + 1)$ <sup>c</sup>Vibrational overlap integrals,  $\langle v' | v'' \rangle$ , and the rotational overlap integrals,  $B_{v',v''}$ , were calculated using Morse potentials for all the states. ( $v' = 0$  and  $v'' = 0$  in most cases, except for matrix elements with  $V^{-1}\Sigma_0^+$ .)

The  $e^3\Sigma^+$  state requires special treatment because it is the only (quasi-) bound state in this energy region that is totally absent from the observed spectra. The  $e^3\Sigma_0^+$  state interacts to first order with the  $d^3\Pi_0$ ,  $d^3\Pi_1$ ,  $G^1\Sigma^-$ , and  $e^3\Sigma_1^+$  states, and the  $e^3\Sigma_1^+$  state interacts to first order with the  $d^3\Pi_0$ ,  $d^3\Pi_1$ ,  $d^3\Pi_2$ ,  $D^1\Pi$ ,  $g^3\Sigma_1^-$ , and  $e^3\Sigma_0^+$  states. To account for the perturbations of the  $\Pi$  states by the  $e^3\Sigma_1^+$  state, which are expected to be manifest mostly in  $\Lambda$ -doubling of these states, we introduced the Van Vleck coefficients<sup>18,19</sup>  $B_0^+$ ,  $B_1^+$ , and  $A_0^+$ ,

$$B_0^+ = \sum_{v'} \langle v, {}^3\Pi | B(R) \mathbf{L}^+ | v', {}^3\Sigma^+ \rangle \\ \times \langle v', {}^3\Sigma^+ | B(R) \mathbf{L}^- | v, {}^3\Pi \rangle / (E_{\Pi} - E_{\Sigma}) \\ = \sum_{v'} (b B_{v,v'})^2 / [8(E_{\Pi} - E_{\Sigma})], \quad (25)$$

$$B_1^+ = B_0^+ + \sum_{v'} \langle v, {}^3\Pi | B(R) \mathbf{L}^+ | v', {}^3\Sigma^+ \rangle \\ \times \langle v', {}^3\Sigma^+ | (\hat{\mathbf{a}}/2) \mathbf{L}^- | v, {}^3\Pi \rangle / (E_{\Pi} - E_{\Sigma}) \\ = B_0^+ + a_+ + b \sum_{v'} B_{v,v'} / [16(E_{\Pi} - E_{\Sigma})], \quad (26)$$

and

$$A_0^+ = \sum_{v'} [\langle v, {}^3\Pi | (\hat{\mathbf{a}}/2) \mathbf{L}^+ | v', {}^3\Sigma^+ \rangle \\ + \langle v', {}^3\Sigma^+ | B(R) \mathbf{L}^- | v, {}^3\Pi \rangle]^2 / (E_{\Pi} - E_{\Sigma}) \\ = \sum_{v'} [2^{-5/2} a_+ + 2^{-3/2} b B_{v,v'}]^2 / (E_{\Pi} - E_{\Sigma}), \quad (27)$$

where  $b$  is defined in Eq. (16) and  $a_+$  is the matrix element of the  $\hat{\mathbf{a}}^+$  operator.<sup>10</sup> The rotational matrix element  $B_{v,v'} \equiv B_{v,S,\Lambda,\Sigma;v',S',\Lambda',\Sigma'} = \langle \Omega \Lambda S \Sigma v | B(R) | \Omega' \Lambda' S' \Sigma' v' \rangle_R$ .<sup>14</sup> These coefficients appear in the matrix elements listed in Table II. We will show that the  $e^3\Sigma_0^+$  state is indirectly characterized through its effect on the  $\Lambda$ -doubling of the  $d^3\Pi_{0,1}$  states. The effect of the spin-orbit interaction of the  $e^3\Sigma^+$  state with the  $g$  and  $G$  states is to shift the term values of the latter by a small  $J$ -independent amount, which is absorbed into the effective term values of these states.

#### IV. RESULTS

The spectroscopic constants were determined by a nonlinear least-squares procedure used previously by Field *et al.*<sup>19</sup> The essential feature of this method is that all of the experimental term values were simultaneously fitted by least-squares adjustment of the free parameters in the effective Hamiltonian matrix. The experimental and fitted term values for HCl and DCl are listed in Tables III and IV, and the optimized set of parameters is listed in Table V. Representative examples of the diabatic state characters are given in Fig. 1 [for the  $V^1\Sigma^+(v'=12)$  state of HCl], and in Tables VI–IX for the  $g^3\Sigma_0^-(v'=0)$  and  $E^1\Sigma^+(v'=0)$  states of HCl and DCl. In all of these examples are seen extensive

$J$ -dependent mixing of the zero-order  $\Sigma$  states. A complete set of tables of diabatic characters for the states that we analyzed are available in the PAPS archive.<sup>20</sup>

We were able to get an overall consistent fit to both the HCl and DCl data. Those parameters which are purely electronic in nature and independent of isotope (namely,  $A_{\Pi}$ ,  $A_{\Delta}$ ,  $a_+$ , and  $b$ ) were taken to be the same for DCl and HCl.  $C_{\Lambda}$ , which is only weakly dependent on the isotope, is also taken to be equal for HCl and DCl; however, as an internal consistency we allowed  $C_{\Pi}$  to vary for both isotopomers. As seen in Table V, the fitted value of  $C_{\Pi}$  for DCl agrees reasonably well with the HCl value ( $-10.1$  vs  $-7.8$   $\text{cm}^{-1}$ ). Some of the parameters which are rotationally dependent (namely,  $B_{1\Sigma^+}$ ,  $B_e$ ,  $D_v$ ,  $D_{3\Sigma^-}$ ,  $\gamma_{\Delta}$ , and  $\gamma_{\Pi}$ ) were held fixed for DCl at values estimated from HCl. In the least-squares fitting procedure, equal weights were assigned to the term values of all levels except for the high rotational levels ( $J' > 7$ ) of the  $D^1\Pi$ ,  $d^3\Pi_0$ , and  $d^3\Pi_2$  states, for which the assignments of Tilford and Ginter<sup>21</sup> are uncertain.

A good test of the fitting procedure is its ability to account for  $\Lambda$ -doubling of the  $\Pi$  and  $\Delta$  states. Figures 2, 3, and 4 compare the experimentally observed  $\Lambda$ -doubling with the calculated values for the  $F^1\Delta_2$  and  $d^3\Pi_1$  states of HCl and the  $d^3\Pi_1$  state of DCl, using a consistent set of parameters for the two isotopomers. Although we succeeded in obtaining a good fit for these states, we could not do so for the higher rotational levels of the  $D^1\Pi_1$ ,  $d^3\Pi_0$ , and  $d^3\Pi_2$  states of HCl. We believe that this failure is due to incorrect assignments by Tilford and Ginter<sup>21</sup> of these high rotational levels. Green *et al.*<sup>22</sup> reported assignments only up to  $J' = 7$  for  $D^1\Pi_1$  and up to  $J' = 4$  for  $d^3\Pi_0$  and  $d^3\Pi_2$ . Also, the observed  $\Lambda$ -doubling of the  $D^1\Pi_1$ ,  $d^3\Pi_0$ , and  $d^3\Pi_2$  states is irregular.

Another possible reason for the poor fit at higher  $J'$  could be a crossing of these states by the  $e^3\Sigma_{0,1}^+$  states. In our model we have introduced the second-order parameters,  $A_0^+$ ,  $B_0^+$ , and  $B_1^+$ , to correct for the fact that we have omitted these states from the Hamiltonian. But this treatment is valid only for  $J$ -levels far from a level crossing with an unseen  $e^3\Sigma_1^+$  level, because we have used nondegenerate perturbation theory to account for the effects of the  $e^3\Sigma_{0,1}^+$  states. The good fit obtained for DCl suggests, however, that this treatment is justified.

From our analysis we find that the electronic assignments of the  $Q(9)$  and  $Q(14)$  rotational lines of the  $G^1\Sigma_0^-$  and  $g^3\Sigma_1^-$  states in the one-photon absorption spectrum reported by Ginter and Ginter<sup>23</sup> should be switched. That is, the line position  $83\,201.76$   $\text{cm}^{-1}$  previously assigned as  $Q(9)$  of  $g^3\Sigma_1^-$  should be assigned as  $Q(9)$  of  $G^1\Sigma_0^-$ , and the line position  $83\,205.88$   $\text{cm}^{-1}$  previously assigned as  $Q(9)$  of  $G^1\Sigma_0^-$  should be assigned to  $Q(9)$  of  $g^3\Sigma_1^-$ . The same  $g \leftarrow G$  reassignment must be made for the  $Q(14)$  lines.

In the following paragraphs we discuss the quantitative values obtained for the various constants in the effective Hamiltonian.

#### A. Spin-orbit constants

From HCl<sup>+</sup> it was found that  $a_{\Pi}$  equals approximately  $-648$   $\text{cm}^{-1}$ .<sup>24</sup> This often quoted value is based on the ( $J$

TABLE III. Measured term values of HCl.<sup>a</sup>

Term values (cm <sup>-1</sup> )							
<i>J'</i>	<i>E</i> <sup>1</sup> Σ <sup>+</sup>	<i>V</i> <sup>1</sup> Σ <sup>+</sup> ( <i>v'</i> =8)	<i>V</i> <sup>1</sup> Σ <sup>+</sup> ( <i>v'</i> =9)	<i>V</i> <sup>1</sup> Σ <sup>+</sup> ( <i>v'</i> =10)	<i>V</i> <sup>1</sup> Σ <sup>+</sup> ( <i>v'</i> =11)	<i>V</i> <sup>1</sup> Σ <sup>+</sup> ( <i>v'</i> =12)	
0	83 780.85	82 226.19	82 839.73	84 333.86	84 207.92	84 747.30	
1	83 793.62	82 232.54	82 847.03	83 444.13	84 216.53	84 755.27	
2	83 819.79	82 245.15	82 862.01	83 465.08	84 234.07	84 771.02	
3	83 859.03	82 264.93	82 883.39	83 497.90	84 260.91	84 794.81	
4	83 911.30	82 288.95	82 912.01	83 548.19	84 297.17	84 826.99	
5	83 976.33	82 320.19	82 946.51		84 344.22	84 867.33	
6	84 053.27	82 357.57	82 987.14		84 403.38	84 913.95	
7	84 141.02	82 400.79	...		84 476.60	84 970.99	
8	84 239.27	82 449.37	83 084.91		84 565.64	85 033.81	
9	843 54.08?	82 504.97	83 142.84		84 672.83		
10		82 565.67			84 797.99?		
11		82 631.78					
12		82 703.09					
<i>J</i>	<i>D</i> <sup>1</sup> Π <sub>1</sub> ( <i>e</i> )	<i>D</i> <sup>1</sup> Π <sub>1</sub> ( <i>f</i> )	<i>d</i> <sup>3</sup> Π <sub>1</sub> ( <i>e</i> )	<i>d</i> <sup>3</sup> Π <sub>1</sub> ( <i>f</i> )	<i>d</i> <sup>3</sup> Π <sub>0</sub> ( <i>e</i> )	<i>d</i> <sup>3</sup> Π <sub>0</sub> ( <i>f</i> )	
0					82 271.30	...	
1	82 509.00	82 509.10	81 792.43	81 792.96	82 290.21	82 291.62	
2	82 548.29	82 548.24	81 831.25	81 832.35	82 327.72	82 329.31	
3	82 607.10	82 606.32	81 889.29	81 891.45	82 384.13	82 385.62	
4	82 684.42	82 684.72	81 966.63	81 969.99	82 459.46	82 460.25	
5	82 781.51	82 781.59	82 063.35	82 067.64	82 553.32	82 554.53	
6	82 897.51?	82 897.52	82 179.34	82 184.91	82 665.62?	82 667.18	
7	83 027.83?	83 031.71	82 314.26	82 321.24	82 798.03?	82 799.17?	
8	83 182.28?	83 185.73	82 468.84	82 476.34	82 948.59?	82 950.10?	
9	83 351.74?	83 357.26	82 641.93	82 650.04	83 118.43?	83 119.09?	
10			82 833.96?	82 842.57		83 307.44?	
11						83 514.12?	
<i>J</i>	<i>F</i> <sup>1</sup> Δ <sub>2</sub> ( <i>e</i> )	<i>F</i> <sup>1</sup> Δ <sub>2</sub> ( <i>f</i> )	<i>d</i> <sup>3</sup> Π <sub>2</sub> ( <i>e</i> )	<i>d</i> <sup>3</sup> Π <sub>2</sub> ( <i>f</i> )	<i>f</i> <sup>3</sup> Δ <sub>2</sub> ( <i>e</i> )	<i>f</i> <sup>3</sup> Δ <sub>2</sub> ( <i>f</i> )	<i>g</i> <sup>3</sup> Σ <sub>0</sub> <sup>-</sup> ( <i>e</i> )
0							83 088.26
1							83 103.23
2	82 909.23	82 909.12	81 652.68	81 652.59	82 079.95	82 080.09	83 133.47
3	82 971.25	82 970.98	81 704.47	81 704.29	82 145.13	82 145.16	83 179.59
4	83 053.67	83 053.32	81 773.39	81 773.89	82 231.17	82 231.35	83 242.83
5	83 156.50	83 156.32	81 860.52	81 861.57	82 338.31	82 338.51	83 322.71
6	83 279.53	83 156.15	81 964.53	81 966.22	82 465.78	82 466.07	83 417.79
7	83 422.66	83 278.82	82 087.63	82 089.79	82 613.59	82 613.84	83 525.11?
8	83 585.61	83 421.90		82 230.45	82 780.53	82 781.77	83 632.43?
9	83 768.93	83 767.26			82 968.16	82 968.54	
10	83 971.00	83 969.19			83 173.50		
11	84 192.99	84 190.18					
12	84 434.29	84 430.59					
13	84 693.92	84 689.85					
14	84 974.26	84 967.69					
15	85 270.58	85 263.94					
16		85 578.43					
<i>J</i>	<i>f</i> <sup>3</sup> Δ <sub>3</sub> ( <i>e</i> )	<i>f</i> <sup>3</sup> Δ <sub>3</sub> ( <i>f</i> )	<i>g</i> <sup>3</sup> Σ <sub>1</sub> <sup>-</sup> ( <i>e</i> )	<i>g</i> <sup>3</sup> Σ <sub>1</sub> <sup>-</sup> ( <i>f</i> )	<i>G</i> <sup>1</sup> Σ <sub>0</sub> <sup>-</sup> ( <i>f</i> )	<i>f</i> <sup>3</sup> Δ <sub>1</sub> ( <i>e</i> )	<i>f</i> <sup>3</sup> Δ <sub>1</sub> ( <i>f</i> )
1			83 289.31		...	82 544.07	82 544.02
2			83 330.98	...	...	82 585.17	82 585.68
3	81 938.40	81 939.62	83 390.88	...	...	82 647.02	82 647.32
4	82 014.89	82 015.14	83 462.72	...	...	82 729.81	82 730.21
5	82 109.43	82 109.47	83 530.52	...	...	82 833.06	82 833.10
6	82 223.09	82 223.15	83 593.17	...	...	...	...
7	82 355.21	82 355.99	83 662.99?	...	...	83 100.72	
8	82 506.31	82 506.86		83 963.77?	...		
9				84 137.11?	84141.23?		
10				84 329.29	84336.53		
11				84 539.69	84547.67		
12				...	84773.69		
13				...	85013.19?		
14				85 278.66?	85265.27?		

<sup>a</sup>Question marks indicate uncertain assignments.

TABLE IV. Measured term values of DCI.

Term values (cm <sup>-1</sup> )							
<i>J</i>	<i>f</i> <sup>3</sup> Δ <sub>2</sub> ( <i>e</i> )	<i>f</i> <sup>3</sup> Δ <sub>2</sub> ( <i>f</i> )	<i>g</i> <sup>3</sup> Σ <sub>0</sub> <sup>-</sup> ( <i>e</i> )	<i>F</i> <sup>1</sup> Δ <sub>2</sub> ( <i>e</i> )	<i>F</i> <sup>1</sup> Δ <sub>2</sub> ( <i>f</i> )	<i>d</i> <sup>3</sup> Π <sub>1</sub> ( <i>e</i> )	<i>d</i> <sup>3</sup> Π <sub>1</sub> ( <i>f</i> )
0			83 134.90				
1			83 143.82			81 798.85	81 800.21
2	...	...	83 161.66	82 940.33	82 940.32	81 820.16	81 820.12
3	82 138.54	...	83 188.17	82 971.25	82 971.45	81 850.28	81 850.97
4	82 180.39	82 180.8	83 223.95	83 012.51	83 012.85	81 891.31	81 892.36
5	82 233.48	...	83 268.62	83 064.34	83 064.34	81 942.38	81 943.90
6	82 297.16	82 297.48	83 322.41	83 125.98	83 126.23	82 003.45	82 005.77
7	82 371.35	82 371.46	83 384.68	83 198.01	83 198.67	82 075.13	82 077.82
8	82 455.80	82 455.92	83 453.29	83 280.45	83 281.25	82 156.45	82 159.60
9	82 551.27	82 550.74		83 372.99	83 373.84	82 248.18	...
10	82 655.49	82 655.87		83 475.60	83 476.50	82 530.32	...
11	82 770.99	82 771.11		83 588.38	83 589.26	82 461.43	82 466.35
12	82 896.15	82 896.87		83 711.44	83 711.95	82 582.93	82 588.97
13	83 031.56	83 032.09		83 844.16	83 844.87	82 714.29	...
14		83 177.83		83 987.23	83 987.24	82 855.15	82 863.61
<i>J</i>	<i>D</i> <sup>1</sup> Π <sub>1</sub> ( <i>e</i> )	<i>D</i> <sup>1</sup> Π <sub>1</sub> ( <i>f</i> )	<i>d</i> <sup>3</sup> Π <sub>2</sub> ( <i>e</i> )	<i>d</i> <sup>3</sup> Π <sub>2</sub> ( <i>f</i> )	<i>f</i> <sup>3</sup> Δ <sub>1</sub> ( <i>e</i> )	<i>f</i> <sup>3</sup> Δ <sub>1</sub> ( <i>f</i> )	<i>E</i> Σ <sub>0</sub> <sup>+</sup>
0							83 948.53
1	82 535.91	82 535.64			82 570.48	82 570.52	83 954.76
2	82 555.84	82 556.64	81 659.23	81 658.19	82 591.91	82 592.07	83 966.52
3	82 586.66	82 586.96	81 686.56	81 686.76	82 623.04	82 623.17	83 983.87
4	82 627.20	82 627.07	81 724.83	81 724.89	82 663.93	82 664.72	84 008.49
5	82 677.84	82 677.52	81 772.79	81 772.83	82 716.57	82 716.14	84 033.94
6	82 738.35	82 738.21	81 830.16	81 830.28	82 778.86	82 779.34	84 074.66
7	82 809.27	82 808.82	81 897.93	81 897.56	82 851.36	82 852.15	84 116.90
8	82 889.86	82 889.86	81 973.98	81 974.38	82 934.708	82 935.13	84 165.46
9	82 980.56	82 980.18			83 027.81	83 028.80	84 179.27
10	83 081.17	83 080.23			83 132.83		84 220.34
11	83 191.12	83 191.70					
12		83 311.93					
<i>J</i>	<i>V</i> <sup>1</sup> Σ <sup>+</sup> ( <i>v</i> '=12)	<i>V</i> <sup>1</sup> Σ <sup>+</sup> ( <i>v</i> '=13)	<i>V</i> <sup>1</sup> Σ <sup>+</sup> ( <i>v</i> '=14)	<i>V</i> <sup>1</sup> Σ <sup>+</sup> ( <i>v</i> '=15)			
0	82 942.20	83 389.40	83 739.10	84 298.20			
1	82 945.85	83 393.84	83 744.83	84 302.53			
2	82 953.06	83 402.18	83 756.38	84 311.18			
3	82 963.80	83 414.17	83 772.79	84 324.12			
4	82 977.92	83 428.92	83 794.80	84 341.69			
5	82 995.24	83 445.35	83 821.12	84 363.57			
6	83 015.54	83 462.13	83 851.86	84 389.94			
7	83 038.58	83 477.67	83 886.23	84 420.87			
8	83 064.05	83 490.11	83 923.54	84 456.54			
9	83 091.60	84 497.72	83 963.02	84 497.87			
10	83 120.84						

=0) term value difference of the *X* <sup>2</sup>Π<sub>3/2</sub> and *X* <sup>2</sup>Π<sub>1/2</sub> ionic cores. From our fitted parameters this quantity has a value of -623.3 cm<sup>-1</sup>. The discrepancy is partially explained by the rotational contribution to the electronic term values of the ion cores for the two spin-orbit states. Inspection of Eqs. (13) and (14) for Ω=1/2 and 3/2 shows that for the ground rotational level the spin-orbit splitting is 2*B* - *a*<sub>Π</sub> and not simply -*a*<sub>Π</sub>. Since *B* ≈ 10 cm<sup>-1</sup>, the spin-orbit part of the <sup>2</sup>Π<sub>1/2</sub>, <sup>2</sup>Π<sub>3/2</sub> ion-core splitting is -628 cm<sup>-1</sup>, in good agreement with the *a*<sub>Π</sub> value of 632 cm<sup>-1</sup> for the Rydberg states determined in our fit (*a*<sub>π</sub> = 2*A*<sub>π</sub>, see Tables II and V).

We can estimate *a*'<sub>Π</sub> of the 4*pπ* Rydberg orbital from *A*<sub>Δ</sub> (*a*'<sub>Π</sub> = 4*A*<sub>Δ</sub> - *a*<sub>Π</sub>, see Table II). This value turns out to be +24.7 cm<sup>-1</sup>. This value is consistent with a very rough estimate obtained independently (see Ref. 15) from *a*'<sub>Π</sub> ≈ *a*<sup>+</sup>/*b* = 47.9 cm<sup>-1</sup>.

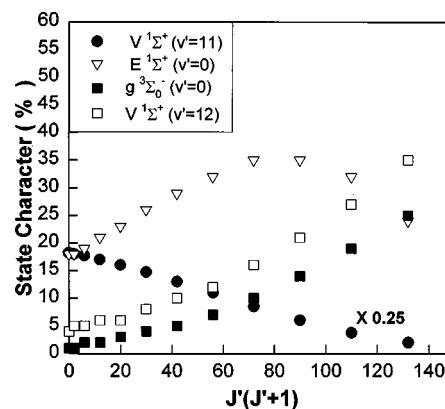
### B. Spin-spin constant

The spin-spin operator is a complicated two-electron operator<sup>10</sup> which represents the interaction energy between the magnetic dipoles associated with the spins of two electrons. Normally the spin-spin interaction constant, η, is very small. (For Cl, η=0.06 cm<sup>-1</sup>, see Ref. 10.) Second-order spin-orbit effects result in matrix elements that have the same form as the spin-spin operator. The large values of effective spin-spin constants that we obtained can be mainly attributed to these second-order spin-orbit effects produced by unseen states not included in the fit.

The spin-spin constants for the <sup>3</sup>Σ<sup>-</sup>, <sup>3</sup>Π, and <sup>3</sup>Δ states can be written as the sum of isoconfigurational and interconfigurational terms.<sup>10,25</sup> Although the dominant contribution within the π<sup>3</sup>π configuration is usually isoconfigurational,

TABLE V. Fitted parameters for HCl and DCI<sup>a</sup>

Parameter	HCl	DCI
$E \ ^1\Sigma_0^+(v'=0)$ ,		
$E_{1\Sigma}$	83 706.9±0.2	83 753.3±1.1
$B_{1\Sigma}$	8.37±0.02	4.18 <sup>b</sup>
$D_{1\Sigma}$	0.004 09±0.000 02	0.0061±0.0003
$V \ ^1\Sigma_0^+$		
$E_{1\Sigma}$	75 820.8±0.1	76 251.3±0.3
$\omega_e$	877.97±0.01	627.39±0.02
$\omega_e x_e$	16.852±0.008	8.161±0.002
$\omega_e y_e$	0.2639±0.0007	0.0628±0.0001
$B_{1\Sigma}$	2.525±0.002	1.289 <sup>b</sup>
$\alpha_e$	-0.0759±0.0001	-0.0449±0.0007
$D_{1\Sigma}$	0.001 76±0.000 01	0.000 011 <sup>b</sup>
$\langle v', V \ ^1\Sigma_0^+   H^{\text{el}}   v'=0, E \ ^1\Sigma_0^+ \rangle$		
HCl		DCI
$H_{E\sim V(8)}$	55±3	0
$H_{E\sim V(9)}$	-117±1	0
$H_{E\sim V(10)}$	187±1	123.7±0.4
$H_{E\sim V(11)}$	-231±1	-140.1±0.7
$H_{E\sim V(12)}$	246±1	
$g \ ^3\Sigma^-(v'=0)$		
$E_{1\Sigma}$	83 263.4±0.2	83 289.2±0.8
$B_0$	9.915±0.006	5.2±0.2
$D_0$	0.0021±0.0001	0.00011 <sup>b</sup>
$C_{\Sigma}$	-5.08±0.15	-5.08 <sup>b</sup>
$\gamma_{\Sigma}$	1.93±0.03	0.96 <sup>b</sup>
$G \ ^1\Sigma^-(v'=0)$		
$E_{1\Sigma}$	83 222.3±0.2	
$B_{1\Sigma}$	10.31±0.01	
$D_{1\Sigma}$	0.0028±0.0002	
$F \ ^1\Delta(v'=0)$		
$E_{1\Delta}$	82 726.6±0.1	82 773.4±0.3
$B_{1\Delta}$	10.046±0.001	5.102±0.004
$D_{1\Delta}$	0.0012±0.000 01	0.000 17±0.000 02
$f \ ^3\Delta(v'=0)$		
$E_{3\Delta}$	822 08.2±0.2	822 44.6±0.4
$B_{3\Delta}$	10.031±0.002	5.176±0.003
$D_{3\Delta}$	0.000 40±0.000 08	0.000 18±0.000 03
$C_{\Delta}$	-3.0±0.2	-3.025 <sup>b</sup>
$\gamma_{\Delta}$	1.00±0.03	0.49 <sup>b</sup>
$A_{\Delta}$	-151.93±0.04	-151.93 <sup>b</sup>
$D \ ^1\Pi(v'=0)$		
$E_{1\Pi}$	82 347.5±0.6	82 391.9±0.4
$B_{1\Pi}$	9.65±0.01	5.012±0.004
$D_{1\Pi}$	0.0004 <sup>c</sup>	0.000 11 <sup>c</sup>
$d \ ^3\Pi(v'=0)$		
$E_{3\Pi}$	81 932.5±0.2	81 949.9±0.2
$B_{3\Pi}$	9.98±0.03	5.097±0.002
$D_{3\Pi}$	0.0004 <sup>c</sup>	0.000 12 <sup>c</sup>
$C_{\Pi}$	-7.8±0.1	-10.1±0.1
$\gamma_{\Pi}$	-2.13±0.04	-1.06 <sup>b</sup>
$A_{\Pi}$	-316.17±0.05	-314.1±0.6
$B_0^+$	-0.272±0.003	-0.0511±0.002
$B_1^+$	-1.74±0.02	-0.78±0.03
$A_0^+$	1.3±0.2	2.89±0.09
$a_+$	34.2±0.9	34.2 <sup>c</sup>
$b$	0.71±0.02	0.71 <sup>c</sup>

<sup>a</sup>All energies are in cm<sup>-1</sup>.<sup>b</sup>The value either equals the HCl parameter or is estimated from the HCl value.<sup>c</sup>The value of this parameter is estimated by assuming a Morse potential energy function.FIG. 1. Diabatic state characters for the  $V \ ^1\Sigma^+(v'=12)$  state of HCl.

contributions from the interaction with the  $\pi^3\sigma$  configuration should also be considered. The isoconfigurational part of the spin-spin constant for  $\Sigma^-$  states is given by<sup>10</sup>

$$C_{\Sigma^-} = -1/3(2A_{\Delta} - 2A_{\Pi})^2 \sum_{v'} |\langle v|v'\rangle|^2 / (E_{3\Sigma^-,v} - E_{3\Sigma^+,v'}). \quad (28)$$

In practice we disregarded contributions to  $v'=0$  from the  $v' \neq 0$  states, assuming that such  $v' \neq 0$  states have negligible vibrational overlaps with  $v'=0$  states. If the  $e \ ^3\Sigma^+$  state lies  $\sim 2000 \text{ cm}^{-1}$  below the  $g \ ^3\Sigma^-$  state, as claimed by Jureta *et al.*,<sup>26</sup> the value of  $C_{\Sigma^-}$  should be  $\sim -17 \text{ cm}^{-1}$ . If the  $e \ ^3\Sigma^+$  state lies close to the  $d \ ^3\Pi$ , as we argue later,  $C_{\Sigma^-}$  would be even more negative. Since the fitted value is  $-5.1 \text{ cm}^{-1}$ , we can attribute the small absolute value of  $C_{\Sigma^-}$  to additional interconfigurational spin-orbit contributions to  $C_{\Sigma^-}$  from states such as  $t \ ^3\Sigma^+$ ,  $a \ ^3\Pi$ ,  $d \ ^3\Pi(v'=1)$ ,  $D \ ^1\Pi_1(v'=1)$  and  $e \ ^3\Sigma^+(v'=1)$ , and also from  $C \ ^1\Pi_1(v'=2,3)$  and  $b \ ^3\Pi(v'=3,4)$ .

The effective spin-spin constant for the  $^3\Pi$  state comes mostly from  $^1\Pi$  states. The isoconfigurational contribution is of the form<sup>10</sup>

$$C_{\Pi} = -1/3(A_{\Pi})^2 \sum_{v'} |\langle v|v'\rangle|^2 / (E_{1\Pi} - E_{3\Pi}). \quad (29)$$

Since the  $D \ ^1\Pi$  state is already included in the model, contributions to  $C_{\Pi}$  in this case are mostly from the  $C \ ^1\Pi(v'=2,3)$ , and  $A \ ^1\Pi$  states.

The effective spin-spin constant for  $^3\Delta$  states comes mostly from  $^1\Delta$  states. This isoconfigurational contribution is of the form<sup>10</sup>

$$C_{\Delta} = -1/3(2A_{\Delta} - 2A_{\Pi})^2 \sum_{v'} |\langle v|v'\rangle|^2 / (E_{3\Delta} - E_{1\Delta}). \quad (30)$$

Typical values for direct spin-spin, as opposed to second-order spin-orbit contributions to the effective spin-spin constants,  $C_{\Pi}$  and  $C_{\Delta}$ , are on the order of  $0.1 \text{ cm}^{-1}$  ( $3\eta$  for  $C_{\Delta}$  and  $-3/2 \eta$  for  $C_{\Pi}$ <sup>10</sup>). Inasmuch as the fitted constants listed in Table V are considerably larger in magnitude, we infer that there must be contributions to the effective spin-spin constants from other configurations.

TABLE VI. Diabatic characters of the states of the  $g^3\Sigma_0^-(v'=0)$  state of HCl.<sup>a</sup>

$J$	Energy (obs.)	Energy (fit)	$g^3\Sigma_0^-(v'=0)$	$E^1\Sigma^+(v'=0)$	$V^1\Sigma^+(v'=9)$	$V^1\Sigma^+(v'=10)$	$g^3\Sigma_1^-(v'=0)$
0	83 088.3	83 088.1	63	22	6	5	0
1	83 103.2	83 103.6	62	22	5	5	<1
2	83 133.5	83 134.3	61	22	5	5	3
3	83 179.6	83 180.8	58	23	4	6	5
4	83 242.8	83 243.2	55	23	3	8	7
5	83 322.7	83 320.8	50	23	2	11	8
6	83 417.8	83 411.5	44	24	2	18	7
7	83 525.1	83 510.0	33	23	2	31	5
8	83 632.4	83 607.7	19	20	1	51	3

<sup>a</sup>Energies are in  $\text{cm}^{-1}$ .

### C. Spin-rotation constants

A rough estimate of the true microscopic value for  $\gamma$  can be made from the equation<sup>10</sup>

$$\gamma \approx -(m/M)A, \quad (31)$$

where  $m/M = 1/1836$ , and  $A$  is the spin-orbit constant for the molecular electronic state. This value of  $\gamma$  is typically  $\sim 0.1 \text{ cm}^{-1}$  for HCl, because  $A \sim 300 \text{ cm}^{-1}$ . It is possible that the effective value of  $\gamma$  could be much larger because of second-order (spin-orbit times rotational) effects. For example, for  $\text{O}_2$  it was found that the experimental value of  $\gamma$  is ten times larger than the calculated microscopic value.<sup>10</sup> For HCl the effective values are also about an order of magnitude larger than the estimated microscopic spin-rotation values. The larger effective values of  $\gamma_{\Pi}$  are caused by second-order **L**- and **S**-uncoupling by states not included in the model, because the matrix elements for these perturbations have the same form  $[\propto (X-2)^{1/2}]$  as that of the spin-rotation operator. These second-order perturbations are of the type  $\mathcal{H}^{\text{ROT}} \times \mathcal{H}^{\text{SO}}$ , such as  ${}^3\Pi_0 \sim {}^3\Delta_1 \sim {}^3\Pi_1$ , where the first interaction is **L**-uncoupling (and therefore  $\Delta S=0$ ), and the second is spin-orbit.

### D. Rotational and centrifugal distortion constants

The effect of deperturbation on the  $B$ -values of the  $E^1\Sigma_0^+$  and  $g^3\Sigma_0^-$  states is clear: As a result of valence state mixing, the  $E^1\Sigma_0^+$  and  $g^3\Sigma_0^-$  states have atypically small

empirical rotational constants ( $6.6$  and  $7.3 \text{ cm}^{-1}$ , respectively, for HCl, and  $2.9$  and  $3.1 \text{ cm}^{-1}$  for DCl). After deperturbation, these values are increased by more than  $2 \text{ cm}^{-1}$ . The  $B$ -values for the deperturbed states are increased because the pure Rydberg states, which have a  $(\sigma^2\pi^3)4p\pi$  configuration, all have similar rotational constants ( $10$  for HCl and  $5 \text{ cm}^{-1}$  for DCl). This is true because all the Rydberg states have potential energy curves that are similar to that of the corresponding  $\text{HCl}^+(X^2\Pi)$  ion core. The small empirical  $B$ -values are due to an **L**-uncoupling interaction with a higher-lying principal perturber. The empirical  $B$ -values for the  $E$  state are reduced because that state is homogeneously perturbed by the  $V$  state, which has a smaller rotational constant.

The estimated value of the centrifugal distortion constants is on the order of  $10^{-4} \text{ cm}^{-1}$ , which is determined from the Kratzer formula  $D = 4B^3/\omega^2$  for a Morse potential function.<sup>13</sup> In comparison, our fitted values for all of the  $\Sigma$  states are on the order of  $10^{-3}$ . This discrepancy could be due to the difficulty in completely deperturbing the  $\Sigma$  state manifold. Although our fitted values are large, they at least have the correct sign. In contrast, values of the centrifugal distortion constants for the  $E^1\Sigma_0^+$  and  $V^1\Sigma_0^+$  states obtained by Green *et al.*<sup>22</sup> using traditional fitting methods were often negative. Such negative values are always caused by neglected perturbation effects rather than by pure centrifugal distortion.

TABLE VII. Diabatic characters of the  $E^1\Sigma^+(v'=0)$  state of HCl.<sup>a</sup>

$J$	Energy (obs.)	Energy (fit)	$E^1\Sigma^+(v'=0)$	$V^1\Sigma^+(v'=11)$	$V^1\Sigma^+(v'=10)$	$g^3\Sigma_0^-(v'=0)$	$V^1\Sigma^+(v'=12)$	$g^3\Sigma_1^-(v'=0)$
0	83 780.8	83 781.7	41	23	16	14	3	0
1	83 793.6	83 794.2	41	24	16	14	3	$\ll 1$
2	83 819.8	83 820.8	40	25	14	15	3	$\ll 1$
3	83 859.0	83 859.8	38	28	12	16	3	<1
4	83 911.3	83 911.6	36	31	9	17	3	<1
5	83 976.3	83 975.9	31	36	7	19	2	1
6	84 053.3	84 051.8	26	42	5	21	2	>1
7	84 141.0	84 139.1	18	48	2	23	2	3
8	84 239.3	84 238.0	9	53	1	26	1	7
9 <sup>b</sup>	84 354.1 <sup>c</sup>	84 352.7	1	52	0	27	0	16

<sup>a</sup>Energies are in  $\text{cm}^{-1}$ .<sup>b</sup>For  $J > 9$ , the  $E$  state character disappears and the  $V^1\Sigma^+(v'=11)$  character dominates.<sup>c</sup>Assignment is uncertain.

TABLE VIII. Diabatic characters of the  $g^3\Sigma_0^-(v'=0)$  state of DCI.<sup>a</sup>

$J$	Energy (obs)	Energy (fit)	$g^3\Sigma_0^-(v'=0)$	$E^1\Sigma^+(v'=0)$	$g^3\Sigma_1^-(v'=0)$	$V^1\Sigma^+(v'=1)$	$V^1\Sigma^-(v'=1)$
0	83 134.9	83 134.1	77	20	<1	<1	<1
1	83 143.8	83 143.3	76	20	<1	<1	<1
2	83 161.6	83 161.5	75	20	1	<1	<1
3	83 188.2	83 188.6	74	20	2	<1	<1
4	83 223.9	83 224.7	72	20	4	<1	<1
5	83 268.6	83 269.6	70	20	6	<1	<1
6	83 322.4	83 322.8	68	20	7	1	<1
7	83 384.7	83 383.9	65	21	8	2	<1
8	83 453.3	83 451.4	60	22	8	6	<1

<sup>a</sup>Energies are in  $\text{cm}^{-1}$ .

The fitted value of  $\alpha_e$  for  $V^1\Sigma_0^+$  is negative. For typical potential energy functions, this vibrational correction to the rotational constant is positive. It is possible, however, for  $\alpha_e$  to be negative when the potential function is more parabolic than the Morse function.<sup>13</sup>

### E. $\Lambda$ -doubling constants, $B_0^+$ , $B_1^+$ , $A_0^+$

Most of the fitted values obtained for DCI are consistent with the values obtained from HCl. The estimated values of  $B_0^+$ ,  $B_1^+$ ,  $A_0^+$  for DCI, calculated from the values for HCl using Eqs. (25)–(27), are  $-0.07$ ,  $-0.73$ , and  $+2.41 \text{ cm}^{-1}$ , respectively. For comparison, the fitted values for DCI listed in Table V are  $-0.05 \pm 0.01$ ,  $-0.78 \pm 0.03$ , and  $2.89 \pm 0.09 \text{ cm}^{-1}$ . The DCI parameters deduced from the HCl spectrum are very close to the values obtained by a direct fit of the DCI spectrum, showing that our deperturbation model, which is based on isotopically independent molecular coupling constants embedded in a model that contains all the isotope effects, is internally consistent.

### F. Electrostatic interaction matrix element between the $E^1\Sigma_0^+$ and $V^1\Sigma_0^+$ states

We can estimate the  $H_{E\sim V}$  electrostatic interaction matrix element from the fitted values of the product  $H_{E\sim V}\langle v'|v\rangle$ . Based on the Franck–Condon overlap integrals calculated assuming Rydberg–Klein–Rees (RKR) potential energy curves for both states, the values of  $H_{E\sim V}$  calculated from  $v'=8-11$  are  $44\,500 \pm 3,400$ ,  $50\,580 \pm 630$ ,

TABLE IX. Diabatic characters of the  $E^1\Sigma^+(v'=0)$  state of DCI.<sup>a</sup>

$J$	Energy (obs.)	Energy (fit)	$E^1\Sigma^+(v'=0)$	$V^1\Sigma^+(v'=14)$	$V^1\Sigma^+(v'=15)$	$g^3\Sigma_0^-(v'=0)$
0	83 948.5	83 946.4	39	43	8	8
1	83 954.7	83 952.8	40	42	8	8
2	83 966.5	83 965.5	41	40	8	8
3	83 983.9	83 984.6	43	36	9	9
4	84 008.5	84 010.1	45	32	11	10
5	84 038.9	84 041.8	46	28	12	11
6	84 074.7	84 079.1	48	24	14	13
7	84 116.9	84 121.6	48	20	16	14
8	84 165.5	84 168.4	47	18	16	16
9	84 220.3	84 219.1	44	13	21	19

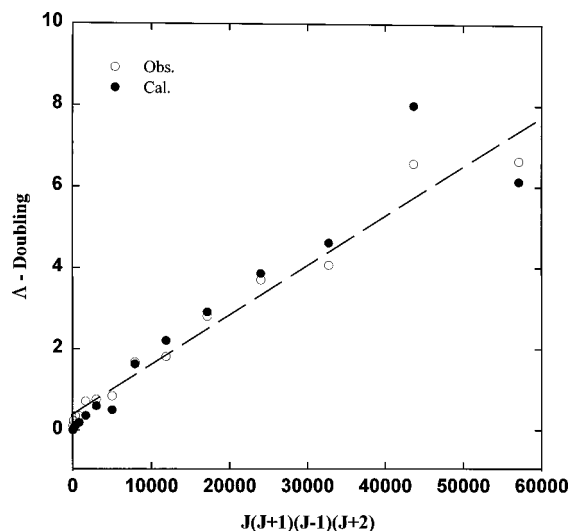
<sup>a</sup>Energies are in  $\text{cm}^{-1}$ .

FIG. 2.  $\Lambda$ -doublings ( $e-f$ ) of the  $F^1\Delta_2$  state of HCl. Open circles are the observed  $\Lambda$ -doublings, and the closed circles are the calculated values. The dashed line is a linear regression.

$56\,570 \pm 300$ , and  $42\,600 \pm 110 \text{ cm}^{-1}$ , respectively. We have not found in the literature a calculated value for this electrostatic interaction, but we can compare it with the reported value for  $\langle A^2\Sigma^+, 4s\sigma | H^{el} | A^2\Sigma^+, \sigma^*3p \rangle = 7000 \text{ cm}^{-1}$ .<sup>27</sup> This interaction involves only a single orbital change, as compared with the two-orbital change for the  $E\sim V$  perturbation. The unrealistically large fitted values of  $H_{E\sim V}$  and their variation with  $v'$  are due entirely to our inability to evaluate accurately the vibrational overlap factors for the  $E^1\Sigma_0^+$  and  $V^1\Sigma_0^+$  states. In order to treat the  $E\sim V$  interaction in the diabatic basis, where the interaction matrix elements can be written as the product of a calculated vibrational overlap and a constant electronic factor,  $H_{12}^e$ , it is necessary to start with diabatic potential curves for the  $E$  and  $V$  states. Even the apparently perturbation-free low- $v$  levels

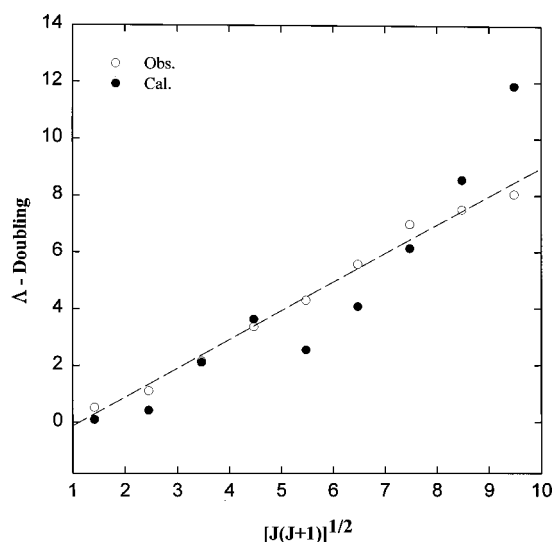


FIG. 3.  $\Lambda$ -doublings ( $f-e$ ) of the  $d^3\Pi_1$  state of HCl. The open circles show the experimental  $\Lambda$ -doublings, and the closed circles show the calculated values. The dashed line is a linear regression.

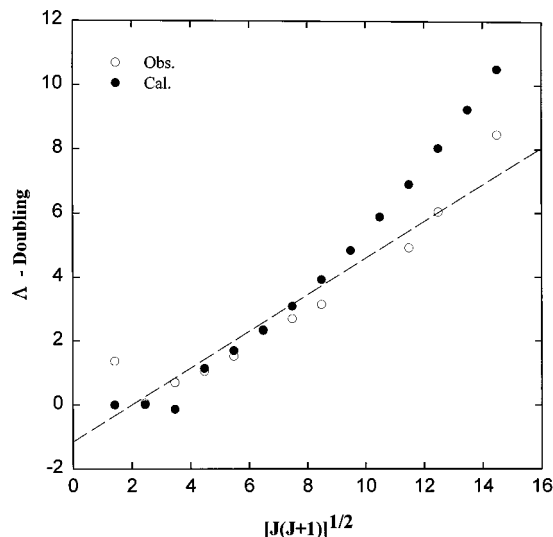


FIG. 4.  $\Lambda$ -doublings ( $f-e$ ) of the  $d^3\Pi_1$  state of DCI. The open circles show the experimental  $\Lambda$ -doublings, and the closed circles show the calculated values. The dashed line is a linear regression.

of the  $V$  state are of mixed  $V\sim E$  diabatic character and cannot be used to derive a diabatic potential unless a global  $V\sim E$  deperturbation is performed. There is certainly a large electrostatic interaction between the diabatic  $V$  and  $E$  states; however,  $H_{12}^e$  is likely to be an order of magnitude smaller than the value derived from our partial  $V\sim E$  deperturbation.

## V. DISCUSSION

From a knowledge of the molecular constants and diabatic state characters it is possible to explain and predict many phenomena. Three examples that we discuss here are the prediction of the energies of unobserved states and explanations of spectroscopic intensity anomalies and of the photodissociation dynamics of predissociating states.

### A. Locating the energy of the $e^3\Sigma^+$ state

The energy of the  $e^3\Sigma^+$  state can be estimated from the fitted values of  $B_0^+$ ,  $B_1^+$ ,  $A_0^+$ , using Eqs. (25)–(27) to solve for  $E_\Sigma$ . From the value of  $B_0^+$ , the  $v'=0$  level of the  $e^3\Sigma^+$  state lies  $23\text{ cm}^{-1}$  above the origin of the  $d^3\Pi$  state; from  $B_1^+$ , it should lie  $10\text{ cm}^{-1}$  above the origin, and from  $A_0^+$  it should lie  $55\text{ cm}^{-1}$  below the origin. The apparent inconsistency of these results can be partially explained by the fact that the  $B_0^+$  and  $B_1^+$  parameters are mostly determined by the  $\Lambda$ -doubling of states with  $\Omega=1$  and  $2$ , whereas  $A_0^+$  is determined mainly by the  $\Lambda$ -doubling for  $\Omega=0$ . The spin-orbit operator splits the  $^3\Pi$  states into three sublevels, and the term values of the  $^3\Sigma^+$  state are referenced with respect to these  $\Omega$  sublevel origins. In a more rigorous treatment, the  $\Lambda$ -doubling constants,  $B_0^+$ ,  $B_1^+$ , and  $A_0^+$ , could be broken down into components corresponding to contributions from individual  $\Omega$  levels of perturbed and perturbing states. The best that we can say from the present analysis is that the origin of the  $e^3\Sigma^+$  state lies near the origin of the zero-order  $d^3\Pi$  state, at an energy of  $81\,860\pm 50\text{ cm}^{-1}$ .

### B. Prediction of the positions of the higher Rydberg states

The effective principal quantum numbers  $n^*$  of the Rydberg states are given by

$$E_R = E_{\text{ion}} - \text{Ry}/n^{*2}, \quad (32)$$

where  $\text{Ry}$  is the Rydberg constant, and  $E_{\text{ion}}$  is the energy of the ion core state. From the values of  $n^*$  obtained for the deperturbed states, one can predict the positions of higher Rydberg states having the same core configuration. For example, we can predict the position of the  $^3\Delta_1$  states which belong to the  $(\sigma^2\pi^3)np\pi$  manifold. The effective quantum number,  $n^*$ , for  $f^3\Delta$  based on Eq. (32) is  $2.3106$ . Hence the predicted deperturbed position of the next higher  $(X^2\Pi)np\pi^3\Delta_1$  state [ $n^*\sim 3.3106, (\sigma^2\pi^3)5p\pi$ ], neglecting rotational interactions and using the same perturbation parameters, is  $\sim 93\,080\text{ cm}^{-1}$ . Similarly, one may predict the energies of other states by diagonalizing the complete Hamiltonian obtained by adding an integer to the deperturbed  $n^*$ -value for each excited Rydberg state and scaling the spin-orbit matrix elements by  $n^{*-3}$ .

### C. Intensity anomalies

In many electronic bands a number of rotational transitions are weak or even missing in the observed spectra. These intensity losses are caused by coupling of the excited state to continuum states or to predissociated bound states. The coupling mechanism can be understood quantitatively by considering the diabatic characters of the interacting states. A well-studied example is the  $F^1\Delta \leftarrow X^1\Sigma^+(0-0)$  transition of HCl.<sup>5-7</sup> The line strengths for transitions to  $J'=2-10$  are anomalously weak. Although the  $F$  state is intersected by the  $t^3\Sigma^+$  continuum state, the two states do not interact in first order.<sup>28</sup> The  $b^3\Pi(v'=3)$  and  $C^1\Pi(v'=2)$  states, however, are known to be strongly predissociated,<sup>9,29,30</sup> and the term values of their rotational levels near  $J'=8$  are very close to those of the  $F^1\Delta(v'=0)$  state. Their interaction with the  $F^1\Delta$  state is further enhanced by the spin-orbit interaction between the  $F^1\Delta$  and  $f^3\Delta$  states. Rotational mixing of the  $F/f$  states with the  $C/b$  states completes the picture. The  $b$  and  $C$  states serve as efficient gateway states, even though the  $\Pi$  characters of the  $F/f$  states are very small. A quantitative model for the intensity anomalies associated with  $F-X(0-0)$  and  $(1-0)$  transitions in both HCl and DCI has been presented.<sup>6</sup> This model was confirmed by the simultaneous detection of neutral Cl atoms produced at the two-photon level and parent molecular ions produced at the three-photon level.

A very different picture emerges for the  $E^1\Sigma^+(0-0) \leftarrow X^1\Sigma^+(0-0)$  transitions of HCl and DCI. The  $E$  state is extensively mixed by electrostatic interaction with many different vibrational levels of the  $V^1\Sigma^+$  valence state and by spin-orbit interaction with the  $g^3\Sigma_0^-$  Rydberg state. We observe experimentally a  $J$ -dependent intensity anomaly for the  $E$  state that differs for HCl and DCI.<sup>7</sup> That is, we find that the resonantly enhanced multiphoton ionization (REMPI) signal for this state is smaller than calculated from the known population of ground state molecules, assuming the usual

two-photon rotational line strength factors. For HCl this intensity loss increases monotonically with  $J$ , whereas for DCI it decreases with  $J$ . These intensity anomalies may be explained by the behavior of superexcited states at the three-photon level. Because the  $V$  state has an  $A^2\Sigma^+$  core, which is much more energetic than the  $X^2\Pi$  ion core, the superexcited state reached by absorption of a third photon can ionize only by electronic autoionization.<sup>10</sup> A kinetic analysis used to model the observed intensity anomalies<sup>7</sup> in the REMPI spectrum of the  $E$ - $X$  transition indicated that electronic autoionization is much slower than predissociation, so that the  $V$  state character at the two-photon level favors the production of neutral three-photon products. The opposite  $J$ -dependences of the intensity anomalies observed for HCl and DCI are explained by their respective diabatic state characters. In Table VII we see that the  $V(v'=10,11)$  character of the  $E$  state increases from 39% to 54% as  $J'$  increases from 1 to 8. This result is consistent with a monotonically increasing intensity anomaly. For DCI, on the other hand, Table IX shows that the  $V$  character of the  $E$  state decreases from 51% for  $J'=0$  to 34% for  $J'=8$ , which is consistent with a monotonically decreasing intensity loss in the REMPI spectrum. The simultaneous production of  $\text{Cl}^+$  and  $\text{HCl}^+$  ions by the pump laser is also explained by this mechanism. Molecules absorbing three pump photons can predissociate to form  $\text{H}+\text{Cl}^*$ , and the electronically excited  $\text{Cl}^*$  atoms are ionized more efficiently by a fourth photon.

A third example is the intensity anomaly of the  $g^3\Sigma_0^-$  state of HCl and DCI.<sup>8</sup> For both isotopomers the intensity loss increases monotonically with  $J'$ . The explanation of this effect is evident in Tables VI and VIII, which show that the  $g^3\Sigma_1^-$  character of these states increases with  $J'$ . The  $g_1$  state is strongly predissociated, presumably by its coupling to the  $C/b$  states.

#### D. Photodissociation dynamics

The recoil angles and internal states of the fragments of a dissociating molecule depend strongly on the diabatic state character of a molecule. This dependence on zero-order character is clearly seen in the predissociation of the  $E^1\Sigma^+(0-0)$  and  $g^3\Sigma_0^-$  states of HCl and DCI.<sup>8</sup> At low  $J'$ , both the  $E$  and the  $g_0$  states predissociate to give primarily  $\text{Cl}(^2P_{1/2})$ , which recoils in a direction parallel to the electric vector of the photon. At  $J'=0$ , the  $g_0$  state gets all of its oscillator strength from its  $E$  and  $V$  state character. All three states have  $0^+$  symmetry ( $e$  parity). The reason for the preponderance of  $\text{Cl}(^2P_{1/2})$  product is that the only continuum state that these states can interact with is the  $a^3\Pi_0^+$  state, which correlates adiabatically with  $\text{Cl}(^2P_{1/2})$  and diabatically with  $2/3 \text{Cl}(^2P_{1/2}) + 1/3 \text{Cl}(^2P_{3/2})$ .<sup>31</sup> The parallel recoil is explained by the  $0^+ - 0^+$  transition from the ground state. For the  $E$  state the  $J$ -dependence of the  $V$  state character does not alter either of these properties. For the  $g_0$  state, however, the increasing  $g_1$  character at higher  $J'$  has a profound effect. The  $g_1$  state gets most of its oscillator strength from the  $C^1\Pi$  state, which predissociates mostly to  $\text{Cl}(^2P_{3/2})$  and undergoes a perpendicular transition from the ground state. Further details are found in Ref. 8.

## VI. CONCLUSION

We have demonstrated in this paper how the complexity apparent in the electronic spectrum and dynamics of a molecule can be explained quantitatively in terms of a minimalist, zero-order electronic structure model. Using HCl/DCI as a test case, a molecular orbital description involving only one electron and one hole was assumed. Coupling matrix elements of different terms of the effective Hamiltonian were expressed analytically in terms of a tractable number of adjustable constants having simple physical significance, which were evaluated by a least-squares fit of the eigenvalues of the Hamiltonian to the observed term values. An overall internally consistent fit of more than 20 vibronic states was obtained for both isotopomers, and the lambda-type doubling for several of these states was well reproduced.

The main result of this analysis is a set of tables listing the fractional contributions of different zero-order states to all the  $v=0$ ,  $J < 14$  Rydberg states of the molecule and their valence perturbers. Using these tables of basis state characters, it is possible to explain many dynamical and spectroscopic properties of the molecule, including intensity anomalies, the  $J$ -dependence of spin-orbit branching ratios of the predissociation products, and the  $J$ -dependence of the angular distributions of the recoiling fragments. Moreover, the zero-order analysis can be used to predict the energies of hitherto unobserved states, in particular that of the  $e^3\Sigma^+$  state.

## ACKNOWLEDGMENT

Support by the National Science Foundation, under Grants No. CHE-94-08801 and PHY-95-27291 (R.J.G.), CHE-96-17418 (R.W.F.), and CHE-91-20339 (R.W.F.) is gratefully acknowledged.

<sup>1</sup>E. F. van Dishoeck, M. C. van Hemert, and A. Dalgarno, *J. Chem. Phys.* **77**, 3693 (1982).

<sup>2</sup>M. Bettendorff, S. D. Peyerimhoff, and R. J. Buenker, *Chem. Phys.* **66**, 261 (1982).

<sup>3</sup>D. S. Ginter and M. L. Ginter, *J. Mol. Spectrosc.* **90**, 177 (1992).

<sup>4</sup>R. Liyanage, Y. Yang, R. J. Gordon, and R. W. Field, *J. Chem. Phys.* **103**, 6811 (1995).

<sup>5</sup>Y. Xie, P. T. A. Reilly, S. Chilukuri, and R. J. Gordon, *J. Chem. Phys.* **95**, 854 (1991).

<sup>6</sup>R. Liyanage, P. T. A. Reilly, Y.-A. Yang, R. J. Gordon, and R. W. Field, *Chem. Phys. Lett.* **216**, 554 (1993).

<sup>7</sup>P. J. Dagdigian, D. F. Varley, R. Liyanage, R. J. Gordon, and R. W. Field, *J. Chem. Phys.* **105**, 10,251 (1996).

<sup>8</sup>A. Strizhev, X. Li, R. Liyanage, R. J. Gordon, and R. W. Field, *J. Chem. Phys.* **108**, 984 (1997).

<sup>9</sup>M. H. Alexander, X. Li, R. Liyanage, and R. J. Gordon, *Chem. Phys.* **231**, 331 (1998).

<sup>10</sup>H. Lefebvre-Brion and R. W. Field, *Perturbations in the Spectra of Diatomic Molecules* (Academic, New York, 1986).

<sup>11</sup>D. R. Yarkony, *J. Phys. Chem.* **100**, 18,612 (1996).

<sup>12</sup>More generally, the diabatic potential energy function is obtained by solving the secular equation  $\det\langle E_i^a(R)|\mathcal{H}^{\text{el}}|E_j^a(R)\rangle - E(R)\delta_{ij} = 0$ , where the solutions  $E(R)$  are either the adiabatic or the Born-Oppenheimer potential energy curves defined in the text. In the latter case,  $H_{12}^a(R)$  has the absolute value  $1/2|V_1^{\text{BO}}(R_C) - V_2^{\text{BO}}(R_C)|$ .

<sup>13</sup>G. Herzberg, *Molecular Spectra and Molecular Structure. I. Diatomic Molecules*, (Van Nostrand, Princeton, 1950).

<sup>14</sup>For brevity, in Tables II and V the vibrational subscripts are omitted from the diagonal matrix elements, and the electronic subscripts are omitted from the off-diagonal ones.

- <sup>15</sup>F. D. Wayne and E. A. Colbourn, *Mol. Phys.* **34**, 1141 (1977).
- <sup>16</sup>Contrary to common usage in the treatment of off-diagonal spin-orbit matrix elements, evaluation of  $l$ -uncoupling  $\mathbf{J}\cdot\mathbf{l}$  matrix elements in an atomic basis set requires special consideration. As discussed in Ref. 15, this difficulty arises from the fact that the centers of mass of the atom and molecule differ. Fortunately, for hydrides this origin-shifting effect is small, though not negligible.
- <sup>17</sup>See p. 98 of Ref. 10. The  $\gamma\mathbf{L}\cdot\mathbf{S}$  part of  $\mathcal{H}^{\text{SR}}$  couples the same states as the rotation-electronic operator and the  $\Delta S=0$  part of the spin-orbit operator, but this effect is very small and is commonly absorbed into the  $a^+$  and  $b$  perturbation parameters.
- <sup>18</sup>K. Freed, *J. Chem. Phys.* **45**, 4214 (1966).
- <sup>19</sup>R. W. Field, B. G. Wicke, J. D. Simmons, and S. G. Tilford, *J. Mol. Spectrosc.* **44**, 383 (1972).
- <sup>20</sup>See AIP Document No. PAPS JCPSA6-109-009839 for 22 pages of tables of diabatic state characters of the electronic states of HCl and DCl. Order by PAPS number and journal reference from American Institute of Physics, Physics Auxiliary Publications Service, 500 Sunnyside Boulevard, Woodbury, New York 11797-2999. Fax: 516-576-2223, e-mail: paps@aip.org. The price is \$1.50 for each microfiche (98 pages) or \$5.00 for photocopies of up to 30 pages, and \$0.15 for each additional page over 30 copies. Airmail additional. Make checks payable to the American Institute of Physics.
- <sup>21</sup>S. G. Tilford and M. L. Ginter, *J. Mol. Spectrosc.* **40**, 568 (1971).
- <sup>22</sup>D. S. Green, G. A. Bickel, and S. C. Wallace, *J. Mol. Spectrosc.* **150**, 388 (1991).
- <sup>23</sup>D. S. Ginter and M. L. Ginter, *J. Mol. Spectrosc.* **90**, 177 (1981).
- <sup>24</sup>D. S. Green and S. C. Wallace, *J. Chem. Phys.* **96**, 5857 (1992).
- <sup>25</sup>R. W. Field, A. Lagerqvist, and I. Renhorn, *Phys. Scr.* **14**, 298 (1976).
- <sup>26</sup>J. Jureta, S. Cvejanović, D. Cvejanović, M. Kurepa, and D. Čubric, *J. Phys. B* **22**, 2623 (1989).
- <sup>27</sup>A. J. Yench, D. Kaur, R. J. Donovan, A. Kvaran, A. Hopkirk, H. Lefebvre-Brion, and F. Keller, *J. Chem. Phys.* **99**, 4986 (1993).
- <sup>28</sup>The interaction between the  $F^1\Delta$  and the  $t^3\Sigma^+$  states is forbidden both because  $\Delta\Lambda=2$  and also because their configurations differ by two orbitals. The latter is also true for the  $b^3\Pi\sim t^3\Sigma^+$  interaction; however, in that case Rydberg-valence mixing in the  $b$  state relaxes this restriction.
- <sup>29</sup>S. G. Tilford, M. L. Ginter, and J. T. Vanderslice, *J. Mol. Spectrosc.* **33**, 505 (1970).
- <sup>30</sup>K. P. Huber and F. Alberti, *J. Mol. Spectrosc.* **97**, 387 (1983).
- <sup>31</sup>M. H. Alexander, B. Pouilly, and T. Duhoo, *J. Chem. Phys.* **99**, 1752 (1993).